THE REACTIVITY OF THE QUINONE METHIDE OF BUTYLATED HYDROXYTOLUENE IN SOLUTION

By

C2011
Maren Gulsrud Willcockson

Submitted to the graduate degree program in
Pharmaceutical Chemistry and the Graduate Faculty of
the University of Kansas in partial fulfillment of the
requirements for the degree of Master's of Science.

Chairperson _____
Valentino J. Stella

Committee Members _____
John Stobaugh

_____
Maria Toteva

Date Defended_____

The Thesis Committee for Maren Gulsrud Willcockson certifies
that this is the approved Version of the following thesis:

THE REACTIVITY OF THE QUINONE METHIDE OF BUTYLATED HYDROXYTOLUENE IN SOLUTION

Chairperson

_____
Valentino J. Stella

_____
Date approved

Acknowledgements

Firstly I'd like thank Dr. Maria Toteva for all her helpful advice, guidance, and patience throughout this project as my adviser in the Pharmaceutics Department at Amgen Inc. I'd also like to acknowledge the teaching, support, and counsel of Dr. Val Stella and the education and assistance I received from the rest of University of Kansas Pharmaceutical Chemistry Department faculty and staff. The support I received from my colleagues at Amgen was deeply appreciated, especially Dr. Mark Ragains for always suggesting the right journal article and everyone who answered my endless questions and gave advice along the way. Lastly I'd like to thank my family and friends, specifically my husband Joseph, for their loving support and kindness and for giving me the encouragement to persevere through the difficulties in life and finish what I started.

Table of Contents

Purpose 1

Introduction 1
- Reactivity of Quinone Methides 2
- A Brief Overview of Literature on the QM from BHT 4
  - Generation 4
  - Toxicity 5
- Specific Aims 6

Experimental, Materials and Methods 7
- Materials 7
- Generation of Quinone Methide (QM) 7
- Determination of QM Concentration 8
- Preparation of Buffer Solutions 8
- pH Measurements 9
- High Performance Liquid Chromatography (HPLC) Analysis 9
- Ultra Violet-Visible Spectrophotometry (UV-Vis) Analysis 9
- Kinetic Studies 10
- Generation of Standard Curves 10
- Calculation of Mole-fractions 11
- Calculation of Rate Constants 11

Results 12
- Modification of the Published Procedure for the Generation of QM 12
- Hydrolysis of QM in Water 13
  - Addition of QM to Water without pH adjustment 13
  - Hydrolysis of QM to BA in the presence of added acid 15
  - Hydrolysis of QM to BA in the presence of added sodium hydroxide 17
- Hydrolysis of QM in the Presence of Chloride Ion 18
- Hydrolysis of QM in the Presence of Phosphate Buffer Species 19
- Reaction of QM in the Presence of Acetate Buffers 20
- Reaction of QM in the Presence of TAPS Buffers 24

Discussion 27
- Hydrolysis of QM to form BA 27
- Hydrolysis of QM in the Presence of Chloride Ion 28
- Hydrolysis of QM in the Presence of Phosphate Buffer 28
- Reaction of QM with Acetate Buffers 30
- Reaction of QM in the Presence of TAPS Buffers 39
- Comparison of QM reactivity to other Quinone Methides 43

Conclusions **47**

References **50**

Appendix: Supplemental Data **55**

Purpose

The purpose of this research is to investigate the kinetic reactivity of the quinone methide of butylated hydroxytoluene, BHT, with some potential nucleophilic buffer species and water, at various pH values and specifically to look for adduct formation.

Introduction

Butylated hydroxytoluene (BHT) is used as an antioxidant in many products including food, pharmaceuticals, cosmetics, jet fuels, rubber, paint, and petroleum products. It is also on the Food and Drug Administration's (FDA) list of compounds generally regarded as safe (GRAS) [1].

The mechanism of action of BHT as an antioxidant is through the formation of a stable phenoxyl radical, which further disproportionates to give the parent and a quinone methide (QM) [2], Scheme 1. Quinone methides are reactive electrophilic species, and easily form adducts with nucleophiles or polymerize. In pharmaceutical formulations, adduct formation between the quinone methide from BHT (QM) and a nucleophilic group of the active pharmaceutical ingredient (API) or another excipient is a very likely possibility. To date there is one report of API-QM adduct formation in a topical formulation [3].

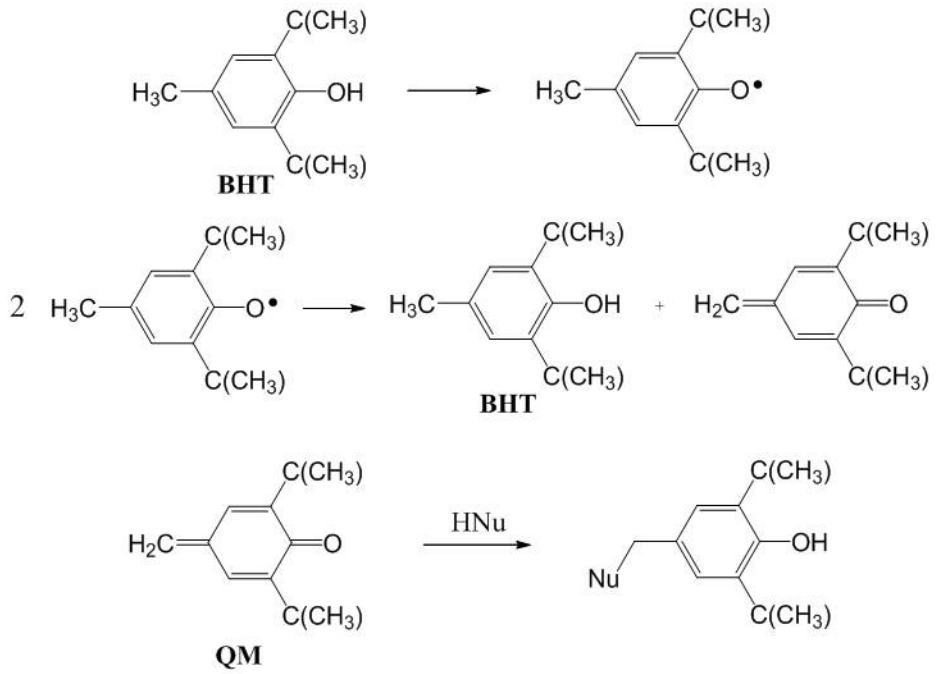

Scheme 1. Reaction pathways for the oxidation of BHT to give QM and the subsequent addition of a nucleophile.

Reactivity of Quinone Methides

Quinone methides can be thought of as charge separated carbocations [4] as depicted in Scheme 2. Effective charges have been calculated for each position of the most simple *p*-quinone methide structure according to the Hückle Molecular Orbital (HMO) model. The effective charge of the methylene carbon is +0.39 and the phenoxyl oxygen has an effective negative charge of-0.68. The 1 and 3 positions of the phenol ring also have a small effective positive charge of +0.18 and +0.11, respectively [5]. This charge distribution characterizes the methylene carbon as the center of nucleophilic reactivity.

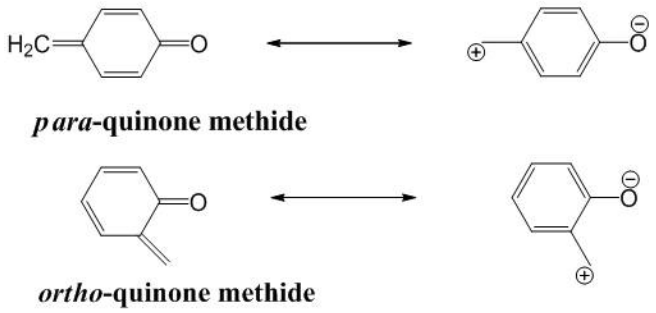

Scheme 2. Resonance structures of *para*- and *ortho*-quinone methides to charge separated carbocations.

The reactivity of quinone methides is further enhanced by the aromatization of the phenyl ring in the product as a result of nucleophilic addition. This provides a strong thermodynamic driving force for addition by nucleophiles to the methylene group. Additional stabilization of the nucleophile adduct is achieved by the protonation of the phenoxyl oxygen in acidic solutions shown in Scheme 3.

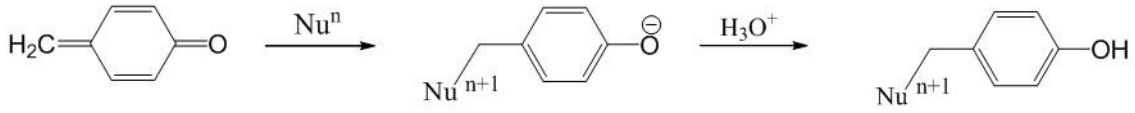

Scheme 3. Reaction pathway for the addition of a nucleophile to a *p*-quinone methide to produce an adduct. The nucleophile adduct is then protonated in an acidic environment.

Both *para*- and *ortho*-quinone methides are used as intermediates in organic and bio-chemistry. The activity of several anti-tumor and antibiotic drugs including tamoxifen [6, 7] and mitomycin C [8] is due to quinone methide formation.

Quinone methides are involved in many biosyntheses. In the natural production of lignin, a copolymer of coniferyl alcohol, the initial coupling of two monomers progresses through a *p*-

quinone methide intermediate [9, 10]. Quinone methides are also proposed intermediates in the biological metabolism of common phenols found in spices [11] through *in vivo* oxidation by cytochrome P-450 [12].

In synthetic chemistry, quinone methides are widely used in Diels-Alder [4+2] cycloaddition reactions with alkenes. This reaction is a key step in the synthesis of large organic molecules including carpanone [13], hexahydrocannabinol [14], and thielocin A1β [15, 16].

There are a variety of known methods to generate quinone methides. Some of them have been reviewed previously, including oxidation of phenols, high temperature dehydration of hydroxybenzyl alcohols, fluoride-induced desilylation of silyl ethers, thermal extrusion of small molecules, and flash photolysis [11]. Due to their high reactivity, quinone methides are also often produced *in situ*.

Brief Overview of Literature on the QM from BHT

Generation

For over half a century chemists have been investigating the properties and reactivity of QM. One of the first reports of the isolation of QM was in the early 1960s. QM was generated at concentrations below 10^{-5} M in isooctane by oxidizing BHT with metal oxides. Another method of generation was the treatment of the corresponding benzyl halide with a base such as triethylamine. At concentrations higher than 10^{-5} M, QM was found to dimerize. A λ_{max} of 285 nm and an extinction coefficient of 2.8×10^4 $cm^{-1}M^{-1}$ were reported [17].

In the 1960s there was disagreement in the literature concerning the mechanism for the oxidation of BHT to QM. Several researchers disagreed on the mechanism of the decay of the phenoxyl radical; the reaction was said to occur through both first and second order kinetics [18,

19]. The mechanism was finally resolved in an experiment where the reaction was followed by ESR Spectrophotometry. The initial time points, from 0 to 500 seconds, appeared to follow first order kinetics. However, after 500 seconds the decay of the radical was clearly second order. The first order appearance of the initial time points was determined to be due to continual formation of the phenoxyl radical by unremoved lead dioxide [2]. Thus QM forms through the second order decay of the phenoxyl radical as shown in Scheme 1.

Toxicity

In 1981 the FDA and several other world regulatory organizations instituted a review of BHT safety as a food additive. This was due to the conflicting scientific evidence in laboratory animals showing both harmful effects in certain tissues and positive effects on lifespan [1]. In the late 1970s studies began to emerge showing toxicity of BHT in rodents [20-24]. Oral dosing of BHT has been shown to cause death in rats from hemorrhaging [21], liver tumors and gastrointestinal tissues [25, 26]. Additionally, lung tissue in mice has been shown to undergo acute damage following intraperitoneal injection [26, 27].

Several of these studies lead to the idea that BHT toxicity comes from the oxidation of BHT to QM [22-24, 28]. *In vivo* BHT has been shown to metabolize through oxidation by cytochrome P-450 to QM [12]. QM has been observed in mouse liver and lung tissue [28] and has also been found to form adducts with glutathione and protein thiols in mouse lung tissue [29]. Similar to other quinone methides [30], QM also forms adducts to DNA *in vitro* [31] and there is some evidence it may also form adducts *in vivo* [32, 33]. *In vitro,* QM has been shown to form a stable thio-ether adduct with cysteine and unstable adducts with lysine and histidine [34].

Specific Aims

BHT is present in pharmaceutical formulations as an antioxidant, however, when oxidized it forms a highly reactive and toxic electrophilic species, a quinone methide. There are a variety of nucleophilic groups present in pharmaceutical formulations as parts of active pharmaceutical ingredients (API), buffers, and excipients that can react with the electrophilic QM.

The specific aims of the this research were to:

1. Investigate the reactivity of the quinone methide of BHT with water under neutral, acidic, and basic conditions and with common buffers at various pH values.
2. Attempt to observe and quantitate adduct formation.
3. Further the general understanding of some of these reactions to lend a greater scientific understanding to the selection of BHT as a pharmaceutical excipient and antioxidant.

QM and adducts formed with nucleophiles in the surrounding environment would be considered degradants and would need to be reported and identified depending on the amount generated. Additionally, very small amounts of these degradants could change the color or odor of the drug product leading to a shorter shelf-life due to perceived or actual adulteration of the product.

Experimental, Materials, and Methods

Materials

Butylated hydroxytoluene (BHT), lead dioxide, and 3, 5-di-tert-butyl-4-hydroxybenzyl alcohol (BA) were purchased from Sigma-Aldrich (St. Louis, MO) and used without additional purification. The following chemicals were reagent grade and purchased from VWR (Radnor, PN): sodium chloride, disodium hydrogen phosphate, and sodium acetate were from JT Baker (Phillipsburg, NJ), sodium dihydrogen phosphate hepta-hydrate was from Mallinckrodt (Phillipsburg, NJ), glacial acetic acid was from EMD (Darmstadt, Germany), while sodium n-tris(hydroxymethyl)methyl-3-aminopropanesulfonate (TAPS) and sodium perchlorate were from Acros (Geel, Belgium). Pentane (EMD), methanol (JT Baker), and acetonitrile (Sigma Aldrich), were HPLC grade, purchased through VWR and Sigma-Aldrich, and were used for all sample preparations and analyses. Water for kinetics studies and HPLC analysis was distilled and passed through a Nano-Pure water purification system.

Generation of Quinone Methide (QM)

QM was generated by modification of a published procedure [35]. A 0.001 M solution of butylated hydroxytoluene (BHT) in pentane containing approximately 25-28 molar equivalents of PbO_2 was stirred at room temperature for 2 hours. Following filtration through a 0.2 μm nylon syringe filter, an equal volume of acetonitrile (ACN) was added and the mixture was rotary evaporated for 1-1 ½ hours at 230 mbar and 40ºC to approximately 35% original volume. The resulting concentrate was added to a volumetric flask and additional acetonitrile was added until the total volume was 10.0 mL. The yield of QM was approximately 30%. The solution was kept

in the freezer for up to 1 week and further diluted for kinetics studies. Unreacted BHT did not appear to interfere with the kinetic analysis.

Determination of QM Concentration

The concentration of quinone methide was determined using total UV absorbance at 285 nm and extinction coefficient values of $\varepsilon_{QM} = 2.82 \times 10^4$ $cm^{-1}M^{-1}$ [2] and $\varepsilon_{BHT} = 2.16 \times 10^3$ $cm^{-1}M^{-1}$ [36] and Equations 1 and 2.

$$Abs_{total} = \varepsilon_{QM} C_{QM} + \varepsilon_{BHT} C_{BHT} \quad \text{(Eq. 1)}$$

$$C_{total} = C^0_{BHT} = C_{BHT} + C_{QM} \quad \text{(Eq. 2)}$$

Preparation of Buffer Solutions

Buffer stock solutions were made at 0.2 M and $I = 1.0$ ($NaClO_4$). Phosphate buffer stock was made by weighing out sodium dihydrogen phosphate, disodium hydrogen phosphate, and sodium perchlorate in appropriate amounts estimated to provide the desired pH value into a 100 mL volumetric flask and dissolving in approximately 80 mL of water. The pH was adjusted with sodium hydroxide and/or perchloric acid to the target pH value. Similarly, acetate buffer stock was prepared from sodium acetate and sodium perchlorate and adding acetic acid in appropriate amounts with the final pH adjusted with sodium hydroxide and/or perchloric acid. TAPS buffer was made by weighting out sodium TAPS and sodium perchlorate and the pH adjusted with perchloric acid. Water was added to reach the target volume and the pH was measured and readjusted if necessary. Lower concentration stock solutions were made by diluting the 0.2 M stock with 1.0 M sodium perchlorate to maintain ionic strength and pH adjusted as above if necessary. Buffers were stored refrigerated for up to a month.

pH Measurements

The pH measurements were performed at ambient conditions using a Thermo Orion 9863BN Needle Tip combination electrode. The electrode was calibrated with three standards, pH 4, 7, and 10, before each series of measurements.

High Performance Liquid Chromatography (HPLC) Analysis

An Agilent 1100 and 1200 Series (Palo Alto, CA) High Pressure Liquid Chromatography—Ultraviolet Spectroscopy (HPLC—UV) instruments each equipped with a binary pump (G1312A), DAD detector (G1315B), auto sampler (G1329A), and 15 x 4.6 mm 5 µm Phenomenex Luna C18 Column were used for the analysis. Elution was performed using a solvent gradient of 40% to 100% B (B = 100% methanol) in solvent A (A = 40% methanol in water) for 20 minutes at a flow rate of 1 mL/min. Peaks were detected at 285 nm and Dionex Chromeleon analysis software (Sunnyvale, CA) was used to integrate peak area.

Ultra Violet-Visible Spectrophotometry (UV-Vis) Analysis

Shimadzu UV-1700 (Japan) Ultra Violet-Visible Spectrophotometer (UV-Vis) equipped with deuterium and halogen lamps was used for sample analysis. For experiments in which the entire spectra were recorded, the spectra were zeroed at 400 nm and scanned from 400 to 190 nm with absorbance values calculated at 285 nm.

Kinetic experiments were followed at 285 nm with sampling time depending on the rate of the kinetic reaction. The data was transferred into excel spreadsheets for analysis. To account for potential drift in the baseline for the long duration runs an empty cuvette was used as a

reference at each time point. Drift was less than 0.004 total absorbance units throughout the experiments so no correction was used.

Kinetic Studies

Kinetic studies were carried out at 25ºC in a 50% (v) aqueous acetonitrile and constant ionic strength, I = 0.5 ($NaClO_4$). Reactions were initiated by mixing equal volumes of aqueous buffer solution and the acetonitrile solution of QM. The final concentration of QM in the reaction mixtures was (1.8 – 4.9) x 10^{-5} M, and the buffer concentration varied from 0.005 to 0.1 M. After initiation, the pH_{app} was measured and aliquots of the reaction mixture were transferred to HPLC vials and incubated in the thermostated HPLC sample holder at 25ºC. In those studies where UV-Vis Spectrophotometry was also used, an additional aliquot was simultaneously transferred to a 1 cm path length quarts cuvette for UV-Vis analysis. For reactions too rapid for HPLC, UV-Vis analysis was used exclusively to monitor the reaction. The reactions were monitored at λ = 285 nm for both the loss of parent and the product formation by HPLC and for total absorbance by UV-Vis.

Generation of Standard Curves

A standard curve for QM was generated by diluting a preparation of QM with acetonitrile 10 to 100 fold and measuring total UV absorbance and HPLC area. The total absorbance was used to calculate the amount of QM at each concentration and this was correlated with the HPLC area to produce a linear standard curve. Chromatograms showed only the presence of QM and BHT and no degradation of QM was observed for the duration of the experiment.

The standard curves for BHT and BA were generated by weighing out different amount of solid standards and dissolving in acetonitrile for UV-Vis and HPLC analysis. The lowest concentrations of BA were prepared by serial dilution in duplicate. The purity listed on the label and volatiles determined by TGA analysis of the standards were corrected for.

Calculation of Mole Fractions

Mole fraction data was calculated using the standard curves for BHT, QM, and BA. The known concentration of each species was subtracted from the total moles of BHT initially used to generate QM; moles unaccounted for were assumed to be the nucleophilic additional product where detected or not accounted for.

Calculation of Rate Constants

Observed first-order rate constants were calculated as the slopes of the semi-logarithmic plots of the HPLC area or change in UV absorbance (absorbance minus absorbance at infinity) against time. Observed second-order rate constants were calculated as the slopes of linear plots of the observed first-order rate constants versus nucleophile concentration. Where necessary, nonlinear curve fitting was performed using Sigma Plot version 11 software (San Jose, CA).

Results

Modification of Published Procedure for the Generation of QM

In a published preparation method for generation of QM, lead dioxide and BHT at a 14:1 PbO_2:BHT molar ratio were stirred in pentane at 25°C for 2 hours [35]. After filtration acetonitrile was added and the pentane removed by evaporation.

Here, QM was prepared based on this procedure, which was modified during initial experiments to yield higher quantities of QM and to remove all residual pentane. In order to maximize the yield of QM, the reaction was followed over the course of 6 hours in pentane by UV spectroscopy, following the change in absorbance at 285 nm. The time course revealed the greatest increase in the concentration of QM between 0 and 2 hours. The concentration of QM continued to grow from 2 hours to 6 hours, however, the slight increase in concentration during this time did not justify the extended experimental time. Therefore, an incubation time of 2 hours was used for all preparations.

The next experimental parameter examined was the amount of lead dioxide. The molar ratio of lead was doubled and tripled to 28:1 and 42:1 respectively, to test the effect of lead concentration on the reaction at the 2 hour time point. It was found that with double the molar ratio of lead dioxide (28:1) QM concentration was significantly increased. Tripling had little increased effect thus a molar ratio of approximately 25-28:1 was used for all preparations.

During initial kinetic studies of the hydrolysis of QM in 50% (v) aqueous acetonitrile I = 0.5 ($NaClO_4$) it was noticed that at the initial time point the HPLC area of the quinone methide was lower than the following time point. Careful observation of the reaction mixtures revealed non-homogeneity, expressed as a thin coating on the vial walls. The coating was assumed to be residual pentane. In order to fully remove all the pentane, evaporation under N_2 was replaced by

evaporation on a rotary evaporator. The pentane-acetonitrile mixture was rotary evaporated at 40 ºC and 235 mbar until the initial volume was reduced to 35%. It was then transferred into a clean volumetric flask and additional acetonitrile added to reach the final volume. After establishing this procedure as routine, pentane was no longer detected in the quinone methide solution and for all experiments described in this work this final method of QM generation was used.

Hydrolysis of QM in Water

In 50% (v) aqueous acetonitrile I = 0.5 ($NaClO_4$) water reacted with QM to form a single product (Scheme 4). The product was identified as the corresponding benzyl alcohol (BA), 3, 5-di-tert-butyl-4-hydroxybenzyl alcohol, by comparison of its HPLC retention time with that of a commercial standard.

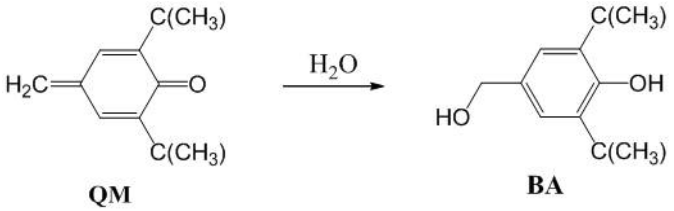

Scheme 4. Addition of water to QM to produce the benzyl alcohol, BA.

Addition of QM to water without pH adjustment

The addition of water to QM was monitored by both HPLC and UV-Vis analysis in 50% (v) aqueous acetonitrile solutions at a constant ionic strength of I = 0.5 ($NaClO_4$) at 25°C. Over the course of the reaction, the disappearance of QM was accompanied by the appearance of BA. A typical chromatogram for this reaction is show in Figure 1. It clearly indicates that QM, the residual BHT, and the water addition product, BA, can all be reasonably separated from one

another. The amount of BHT contamination in the QM solution remains unchanged throughout the course of the reaction.

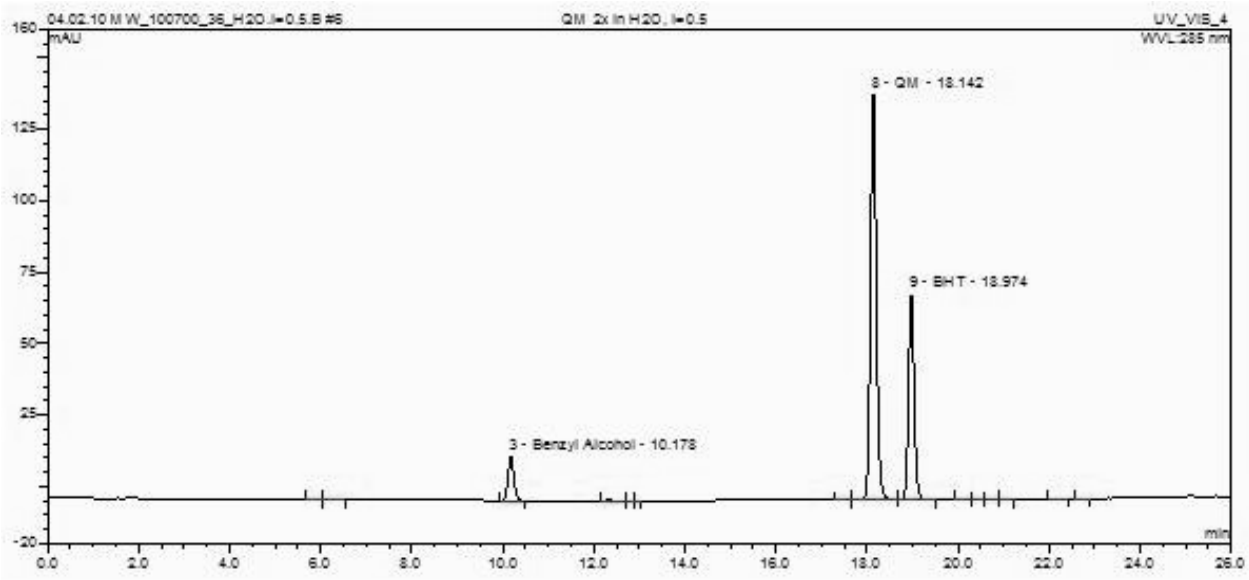

Figure 1. HPLC Chromatogram of the reaction of QM with water in 50% (v) acetonitrile *I* = 0.5 ($NaClO_4$) without pH adjustment and the formation of the benzyl alcohol product, BA, at 25°C.

Figure 2 shows a linear semi-logarithmic plot of the loss of the QM versus time, which indicates the observed order of the reaction is pseudo-first order. The observed first-order rate constant for the disappearance of the QM, obtained from the slopes of these plots, was k_{obs} = (5.33 ± 0.28) x 10^{-2} hr^{-1} (average of 5 runs, Table 1). The measured apparent pH (pH_{app}) of the solutions at the end of the reactions was 7.2 ± 0.1.

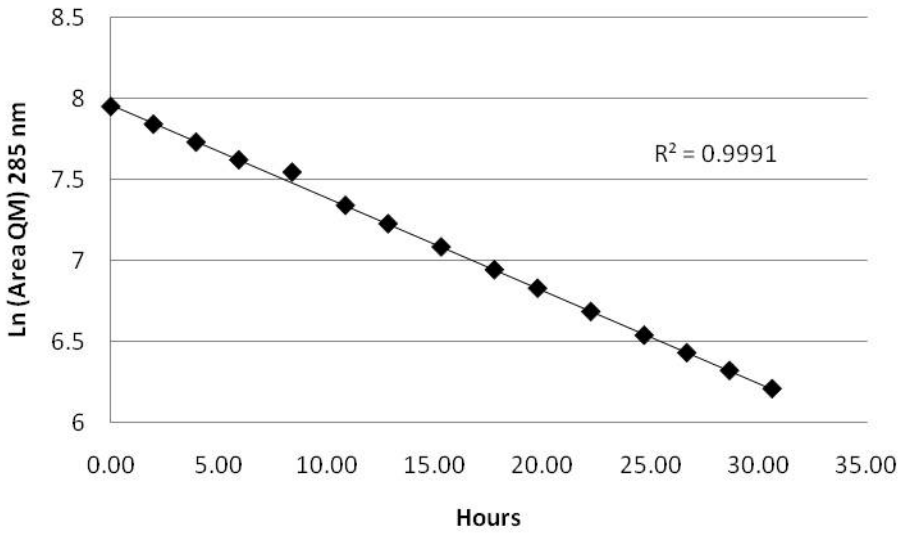

Figure 2. A semi logarithmic plot of the loss of the QM versus time. Data for 1.75 x 10^{-5} M QM (♦) in 50% (v) aqueous acetonitrile *I* = 0.5 ($NaClO_4$) at 25°C.

Table 1. Observed first-order rate constant values, k_{obs}, for hydrolysis of QM in 50% (v) aqueous acetonitrile *I* = 0.5 ($NaClO_4$) to BA followed by HPLC at 25°C. Observed rate constants were calculated as the slopes of the semi-logarithmic plots of the loss of HPLC area at 285 nm versus time.

QM (M)	4.71 x 10^{-5}	2.56 x 10^{-5}	2.93 x 10^{-5}	2.78 x 10^{-5}	1.75 x 10^{-5}
pH_{app}	7.35	7.09	7.16	7.11	7.20
k_{obs} (hr^{-1})	5.37 x 10^{-2}	5.36 x 10^{-2}	5.08 x 10^{-2}	5.08 x 10^{-2}	5.75 x 10^{-2}

Hydrolysis of QM to BA in the presence of added acid

The addition of water to QM in acidic solutions is rapid and was followed by UV spectroscopy as HPLC analysis is too slow to capture the reaction kinetics. The reactions were carried out in solutions containing 0.001 – 0.02 M hydrochloric or perchloric acid. Table 2 summarizes the observed first-order rate constant values, k_{obs} at various acid concentrations. At all concentrations of added acid the reaction followed pseudo-first order kinetics and observed

rate constants were calculated from plotting the logarithm of the loss of UV absorbance at 285 nm versus time.

Table 2. Observed first-order rate constant values, k_{obs} at various added acid concentrations in 50% (v) aqueous acetonitrile I = 0.5 ($NaClO_4$) for reactions followed by UV-Vis at 25°C. Observed rate constants were calculated as the slopes of the semi-logarithmic plots of the loss of UV absorbance at 285 nm versus time.

$[H^+]$ (M)	0.001	0.005		0.0075	0.010		0.015	0.020
Acid	$HClO_4$	$HClO_4$	HCl	$HClO_4$	$HClO_4$	HCl	HCl	HCl
k_{obs} (hr^{-1})	2.35	13.2	13.2	20.1	27.2	26.1	42.1	56.8

Figure 3 shows the dependence of the observed first-order rate constants for the acid catalyzed addition of water to QM on the concentration of acid. The plot is linear and shows strong dependence of the loss of QM on acid concentration and no dependence on counter ion (chloride versus perchlorate). This plot would be expected to have a positive intercept, however, the small negative intercept is likely a result of data variability and error in the extrapolated value. The observed second-order rate constant for the acid catalyzed addition of water to QM, k_H, was calculated as the slope of this plot, $k_H = 2.87 \times 10^3\ hr^{-1}\ M^{-1}$.

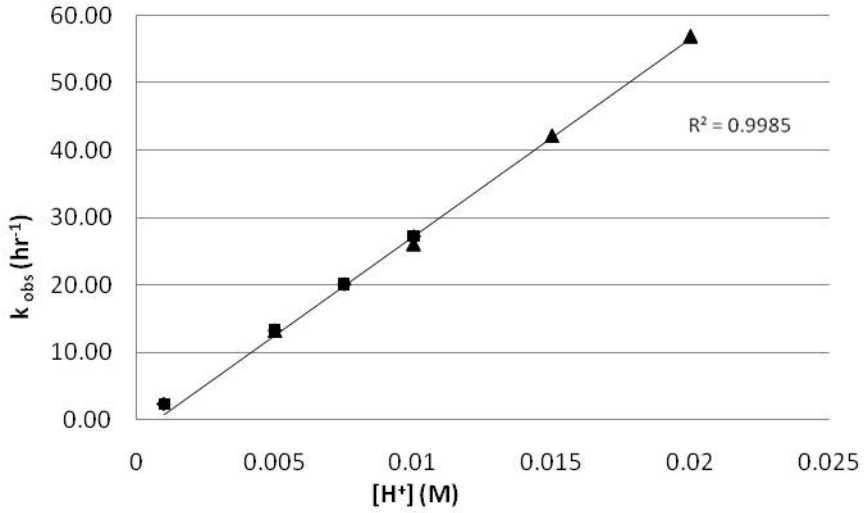

Figure 3. Dependence of the observed first-order rate constants for the hydrolysis of QM on concentration of added acid. Data for hydrochloric acid (▲) and perchloric acid (■) in 50% (v) aqueous acetonitrile *I* = 0.5 ($NaClO_4$) at 25°C.

Hydrolysis of QM to BA in the presence of added sodium hydroxide

The hydrolysis of QM in basic pH solutions with added sodium hydroxide (0.005 – 0.02 M) is rapid and was followed by UV spectroscopy as HPLC analysis is too slow to capture the reaction kinetics. Table 3 summarizes the observed first-order rate constant values, k_{obs} at various hydroxide concentrations. At all concentrations of added base the reaction followed pseudo-first order kinetics and observed rate constants were calculated from plotting the logarithm of the loss of UV absorbance at 285 nm versus time.

Table 3. Observed first-order rate constant values, k_{obs} at various concentrations of sodium hydroxide in 50% (v) aqueous acetonitrile *I* = 0.5 ($NaClO_4$) for reactions followed by UV-Vis at 25°C. Observed rate constants were calculated as the slopes of the semi-logarithmic plots of the loss of UV absorbance at 285 nm versus time.

[OH^-] (M)	0.005	0.010	0.015	0.020
k_{obs} (hr^{-1})	0.50×10^{-1}	1.07×10^{-1}	1.61×10^{-1}	2.10×10^{-1}

Figure 4 shows the dependence of the observed first-order rate constants for the apparent base catalyzed addition of water (or hydroxide ions) to QM on the concentration of added hydroxide. The plot is linear and shows strong dependence of the loss of QM on hydroxide concentration. This plot would be expected to have a positive intercept, however, the small negative intercept is likely a result of data variability and error in the extrapolated value. The observed second-order rate constant for the base catalyzed addition of water to QM, k_{OH}, was calculated as the slope of this plot, $k_{OH} = 11.1\ hr^{-1}\ M^{-1}$.

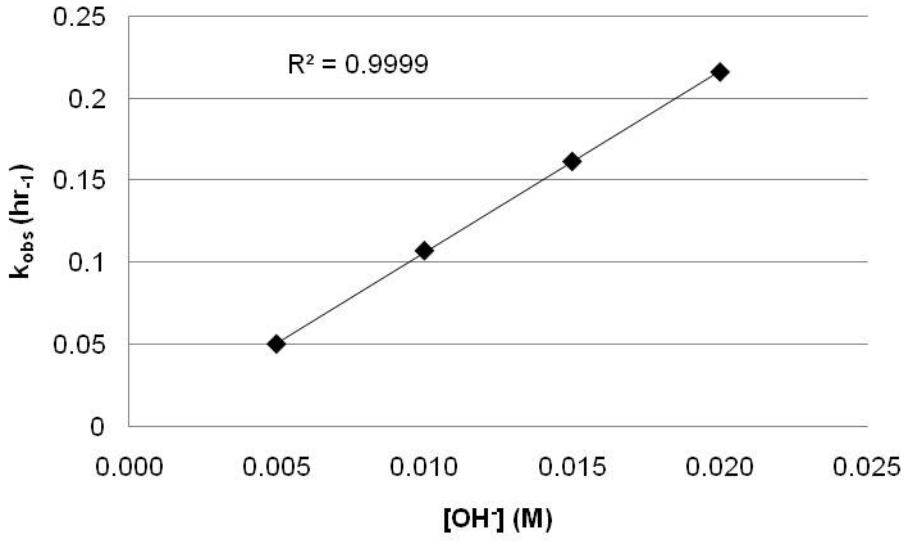

Figure 4. Dependence of the observed first-order rate constants for the hydrolysis of QM on concentration of added hydroxide. Data for sodium hydroxide (♦) in 50% (v) aqueous acetonitrile *I* = 0.5 ($NaClO_4$) at 25°C.

Hydrolysis of QM in the Presence of Chloride Ion

The reaction of QM in the presence of added chloride ion was examined at three concentrations of sodium chloride ranging from 0.05 to 0.1 M and monitored by HPLC analysis.

Reactions were first order with respect to the loss of QM and the observed pseudo-first order rate constants are summarized in Table 4.

Table 4. Observed first-order rate constant values for the reaction of QM in the presence of added sodium chloride, k_{obs} in 50% (v) aqueous acetonitrile I = 0.5 ($NaClO_4$) for reactions followed by HPLC at 25°C. Observed rate constants were calculated as the slopes of the semi-logarithmic plots of the loss of HPLC area at 285 nm.

$[Cl^-]$ (M)	0.050	0.075	0.100
pH_{app}	7.2	7.5	7.8
k_{obs} (hr^{-1})	4.73×10^{-2}	4.84×10^{-2}	4.82×10^{-2}

Chromatograms for the reaction in the presence of added sodium chloride showed no additional product peaks besides the water addition product, BA, and approximate mass balance was observed throughout the course of the reaction.

Hydrolysis of QM in the Presence of Phosphate Buffer Species

The reaction of QM in the presence of phosphate buffer was examined at three concentrations ranging from 0.005 to 0.05 M and monitored by HPLC analysis. At the apparent pH values studied the buffer species present are mono- and dibasic phosphate. Reactions were first order with respect to the loss of QM and the observed pseudo-first order rate constants are summarized in Table 5.

Table 5. Observed first-order rate constant values for the reaction of QM in the presence of phosphate, k_{obs} in 50% (v) aqueous acetonitrile I = 0.5 ($NaClO_4$) for reactions followed by HPLC at 25°C. Observed rate constants were calculated as the slopes of the semi-logarithmic plots of the loss of HPLC area at 285 nm.

[Phos] (M)	0.005	0.025	0.050
pH_{app}	7.40	7.28	7.20
k_{obs} (hr^{-1})	5.37×10^{-2}	5.18×10^{-2}	4.83×10^{-2}

Chromatograms for the loss of QM in the presence of phosphate showed no additional product peaks (including any obvious perturbations at the solvent front) besides the water addition product, BA, throughout the course of the reaction. Extrapolation to t = 0 using the first order rate constant revealed the initial concentration of QM is the same as that in an acetonitrile QM standard, within the error of the measurement, and approximate mass balance was observed. The solubility of phosphate buffer in 50% (v) aqueous acetonitrile in the pH range of interest prohibited testing the reactivity at higher concentrations or higher pH values of phosphate buffer.

Reaction of QM in the Presence of Acetate Buffers

The reaction of QM in sodium acetate buffers was studied at three concentrations ranging from 0.05 M to 0.1 M acetate at pH_{app} values of 4 and 5. A typical chromatogram for the reaction of the QM with acetate buffer is show in Figure 5.

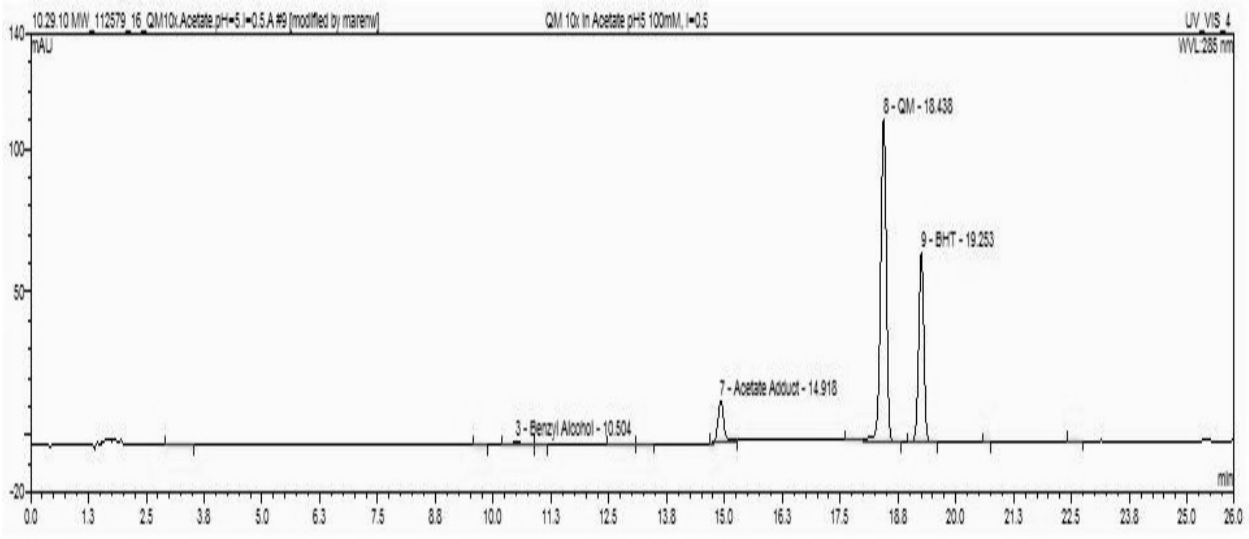

Figure 5. HPLC Chromatogram of the reaction of QM with acetate buffer at pH 5 in 50% (v) acetonitrile *I* = 0.5 (NaClO4) and the formation of the acetate adduct and BA at 25°C.

The HPLC data for the loss of QM and the appearance of products displayed in mole fractions over time at all concentrations and both pH_{app} 4 and 5 is shown in Figures 6 and 7. Two products were observed over the course of the reaction, an unstable presumed acetate adduct and BA. The acetate adduct formed rapidly at early reaction times and slowly converted to BA with time. The initial amount of the acetate adduct was dependent on the total concentration of acetate and pH_{app}. Higher amounts were formed in solutions containing higher concentrations of acetate. The reaction with acetate did not follow simple first order kinetics. The treatment of the kinetic data is described in the discussion.

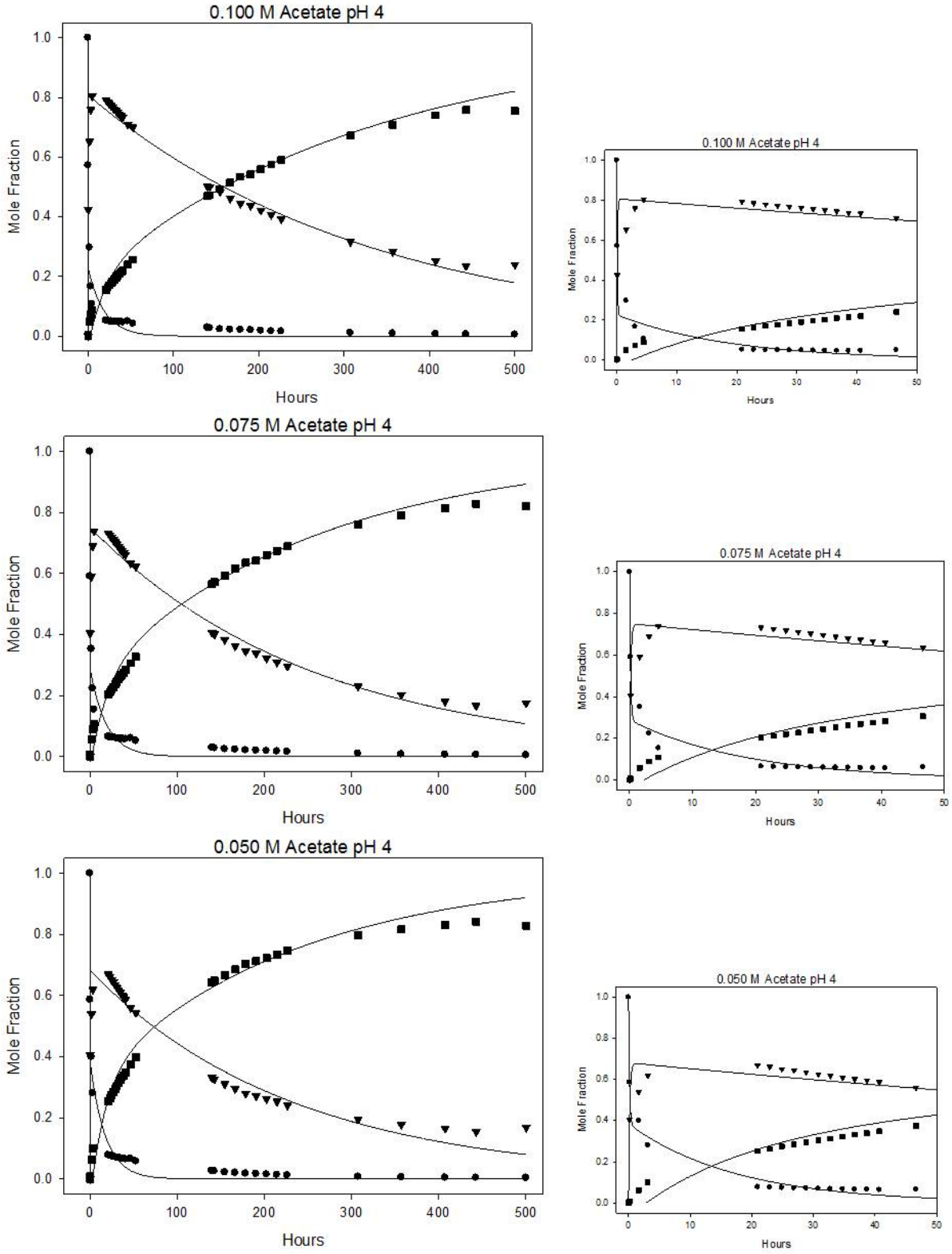

Figure 6. Time course of the reaction of QM in 0.100 – 0.050 M acetate buffer, pH 4. Experimental data points displayed in mole fraction of QM (●), BA(■), and presumed acetate adduct (▼) in 50% (v) aqueous acetonitrile I = 0.5 ($NaClO_4$) at 25°C. Solid lines are the theoretical curves calculated using equations 9-13.

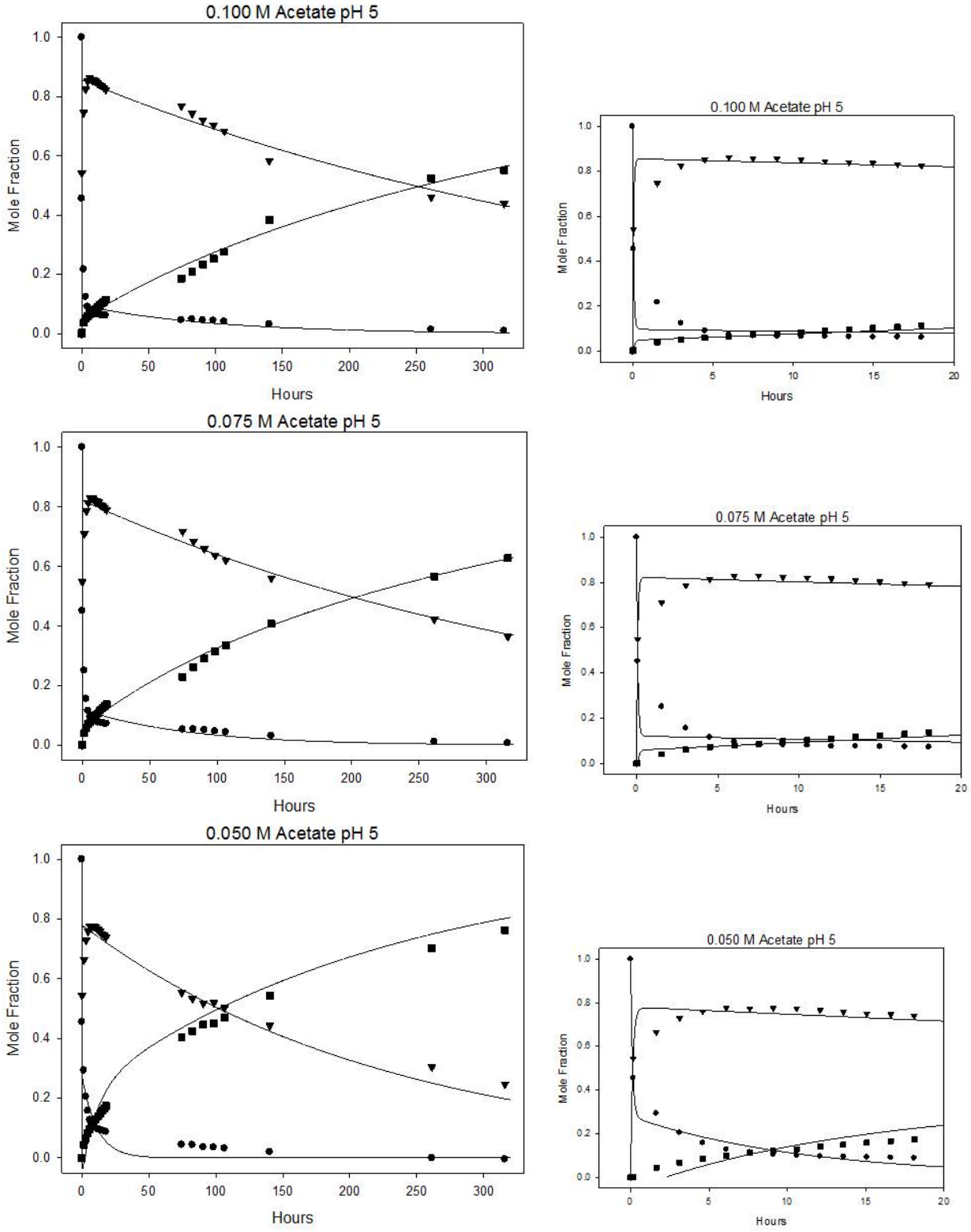

Figure 7. Time course of the reaction of QM in 0.100 – 0.050 M acetate buffer, pH 5. Experimental data points displayed in mole fraction of QM (●), BA(■), and presumed acetate adduct (▼) in 50% (v) aqueous acetonitrile I = 0.5 ($NaClO_4$) at 25°C. Solid lines are the theoretical curves calculated using equations 9-13.

Reaction of QM in the Presence of TAPS Buffers

The reaction of QM in the presence of TAPS buffers was studied at three concentrations ranging from 0.05M to 0.1 M at pH_{app} values 8 and 9. No addition product peaks, including any obvious perturbations at the solvent front, were detected aside from the water addition product, BA.

Similar to the reaction with acetate buffers, the reaction of QM with TAPS buffers did not follow simple first order kinetics. The HPLC data for the loss of QM and the appearance of products displayed in mole fractions over time at both pH_{app} 8 and 9 is shown in Figures 8 and 9. The sum of the moles of QM and BA at each time point did not account for all the moles of QM initially in the reaction; a significant portion of the moles could not be accounted for by peaks in the chromatogram.

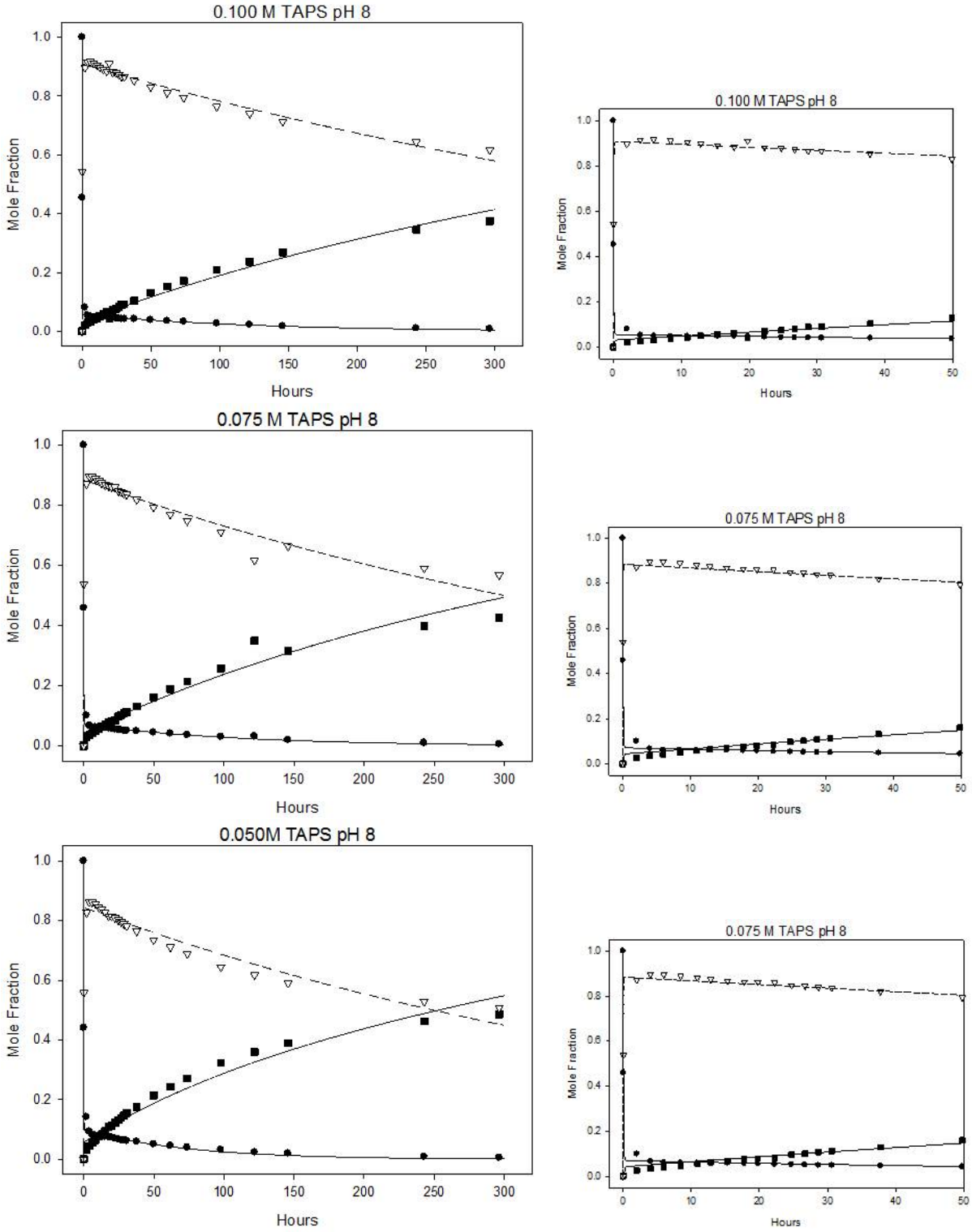

Figure 8. Time course of the reaction of QM in 0.100 – 0.050 M TAPS buffer, pH 8. Experimental data points displayed in mole fraction of QM (●), BA(■), and moles unaccounted for (Δ) in 50% (v) aqueous acetonitrile *I* = 0.5 ($NaClO_4$) at 25°C. Solid and dashed lines are the theoretical curves calculated using equations 9-13.

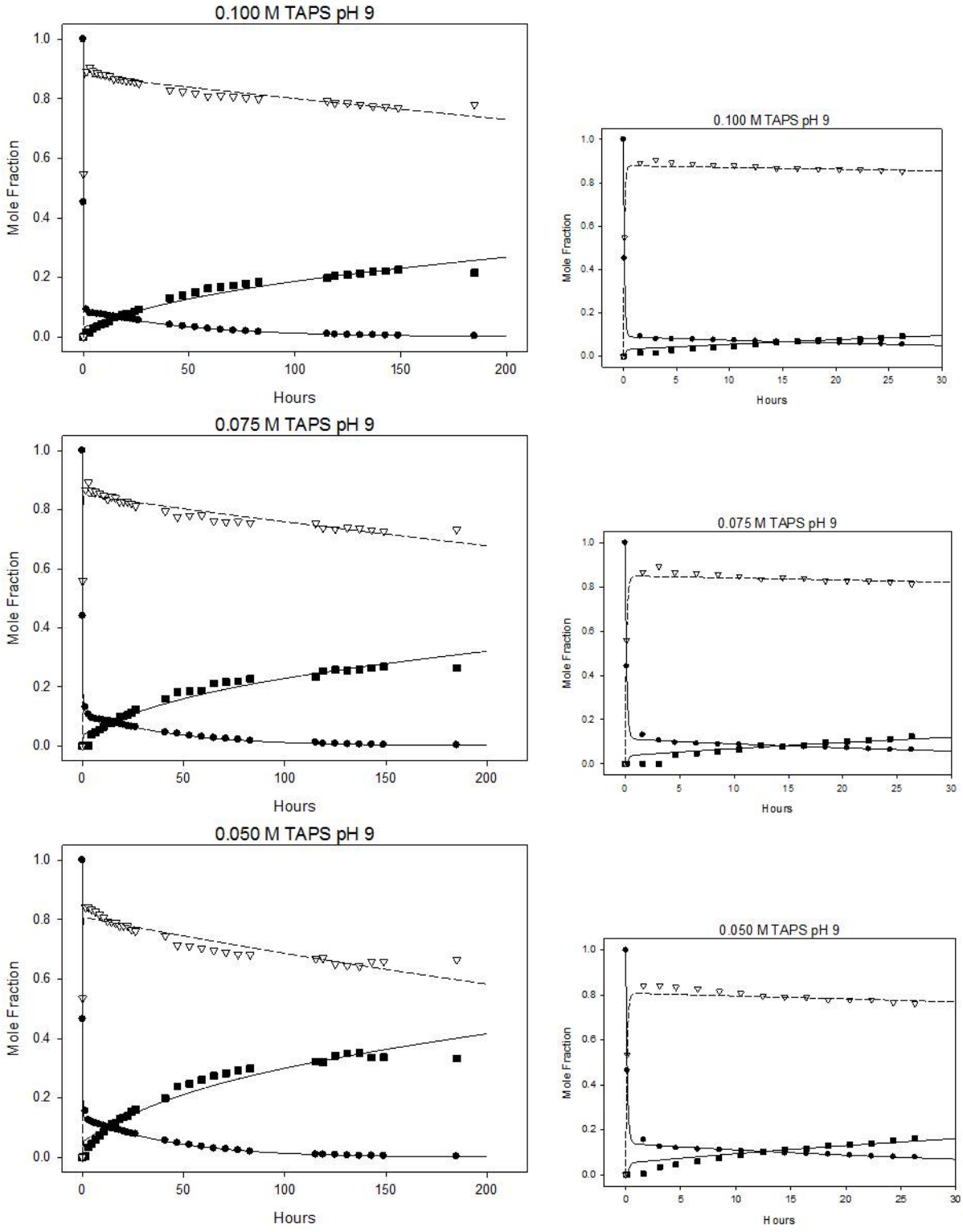

Figure 9. Time course of the reaction of QM in 0.100 – 0.050 M TAPS buffer, pH 9. Experimental data points displayed in mole fraction of QM (●), BA(■), and moles unaccounted for (Δ) in 50% (v) aqueous acetonitrile I = 0.5 ($NaClO_4$) at 25°C. Solid and dashed lines are the theoretical curves calculated using equations 9-13.

Discussion

Hydrolysis of QM to form BA

The hydrolysis of QM to form BA was studied in unbuffered solutions with pH_{app} 7.1-7.4 and at QM concentrations of (1.8 - 4.7) x 10^{-5} M. The addition of water followed simple first order kinetics with an average value of k_s = (5.33 ± 0.28) x 10^{-2} hr^{-1}. Small changes in the initial concentration of QM and pH had no discernable effect on the kinetics.

As reported, the conversion of QM to BA was catalyzed by both the addition of acid and base. The observed first-order rate constants appear to be described by Equation 3, where k_s is the rate of the uncatalyzed addition of water, $k_H[H^+]$ is the contribution of a acid catalyzed reaction, and $k_{OH}[OH^-]$ is the contribution of a base catalyzed reaction. k_H and k_{OH} are the corresponding observed second-order rate constants for the acid and base catalyzed reactions, respectively.

$$k_{obsd} = k_s + k_H[H^+] + k_{OH}[OH^-] \qquad \text{(Eq. 3)}$$

The acid catalyzed addition of water to the QM to form the benzyl alcohol is a very rapid reaction. Followed by UV-Vis the reaction gave simple first-order kinetics throughout the acid concentration range examined regardless of the counter ion. The data gave an observed second-order rate constant k_H of 2.87 x 10^3 M^{-1} hr^{-1}.

The base catalyzed addition of water to the QM to form the benzyl alcohol is also a very rapid reaction. Followed by UV-Vis the reaction gave simple first-order kinetics throughout the hydroxide concentration range examined. The data gave an observed second-order rate constant k_{OH} of 11.1 M^{-1} hr^{-1}.

At neutral pH (corresponding to approximately the reaction kinetics carried out in unbuffered solutions) the effective contribution of the acid and base catalyzed reactions accounts for only 0.5% of the observed first-order rate constant, k_s. Therefore, the uncatalyzed addition of water is a significant kinetic pathway. If a pH-rate profile of the hydrolysis of QM to BA were to be constructed from this data, it would show a plateau from approximately pH_{app} 6-10.

Hydrolysis of QM in the Presence of Chloride Ion

Chloride is a common ion found in many pharmaceutical preparations as an API salt counter ion or used to control the ionic strength of the solution. Followed by HPLC the reaction gave simple first-order kinetics throughout the sodium chloride concentration range examined. An increase in the concentration of sodium chloride from 0.5 to 0.1 M lead to only a 2% difference in the observed first-order rate constants for the reaction, $k_{obs} = 4.73 \times 10^{-2}$ hr^{-1}. A single product was observed throughout the course of the reaction, the benzyl alcohol, BA, and approximate mass balance was observed.

The observed first-order rate constants are also within 10% of the rate of the addition of water without added chloride, $k_s = 5.33 \times 10^{-2}$ hr^{-1}. This difference is slightly outside the expected error for these measurements, and can be perhaps attributed to a non-specific ion effect.

Hydrolysis of QM in the Presence of Phosphate Buffer

Phosphate buffers are commonly used in pharmaceutical formulations. Followed by HPLC, the hydrolysis of QM followed first-order kinetics throughout the phosphate buffer concentration range examined with a single product, BA, observed. Mass balance was seen and extrapolation to $t = 0$ using the observed first order rate constant revealed the initial

concentration of QM is the same as that in an acetonitrile QM standard, within the error of the measurement.

The pH_{app} values of these reaction solutions at different concentrations of phosphate differ by 0.2 pH units. Using the observed second-order rate constants for acid and base catalysis it is possible to take into account the possible contributions of acid and base catalysis but not the contributions from general acid and base catalysis by the mono- and dibasic phosphate species. Thus the observed rate constants for phosphate are reported as measured at each pH_{app} value.

An increase in the concentration of phosphate buffer from 0.005 to 0.05 M lead to a 10% decrease in the observed first-order rate constants for the reaction, k_{obs} = 5.37 x 10^{-2} hr^{-1}. The observed first-order rate constants show a slight trend of increasing rate with decreasing phosphate concentration indicating a possible inverse dependence of the loss of QM on phosphate buffer concentration.

The small effect on rate and the shift in equilibrium of phosphate species, from a change in pH_{app} of 0.2, makes it difficult to generalize about the effect of phosphate buffer concentration or the relative reactivity of either phosphate species on the rate of the loss of QM without additional experimentation. Unfortunately further concentrations and higher pH values for phosphate buffer could not be studied due to the low solubility of phosphate species in 50% (v) aqueous acetonitrile.

The observed first-order rate constants are also within 10% of the rate of the addition of water without phosphate buffer present, k_s = 5.33 x 10^{-2} hr^{-1}. This difference is slightly outside the expected error for these measurements. A non-specific ion effect on the rate for addition of water caused by both phosphate species is possible.

Reaction of QM with Acetate Buffers

Acetate is a common pharmaceutical excipient often used in formulations as a buffering agent. The reaction of QM in the presence of acetate buffer shows an initial decrease in total absorbance that is very rapid compared to the reaction with water. The initial decrease in total absorbance for the acetate buffer reaction is approximately 4 to 8 times faster than the reaction with water depending on pH_{app} and buffer concentration (Figure 10.)

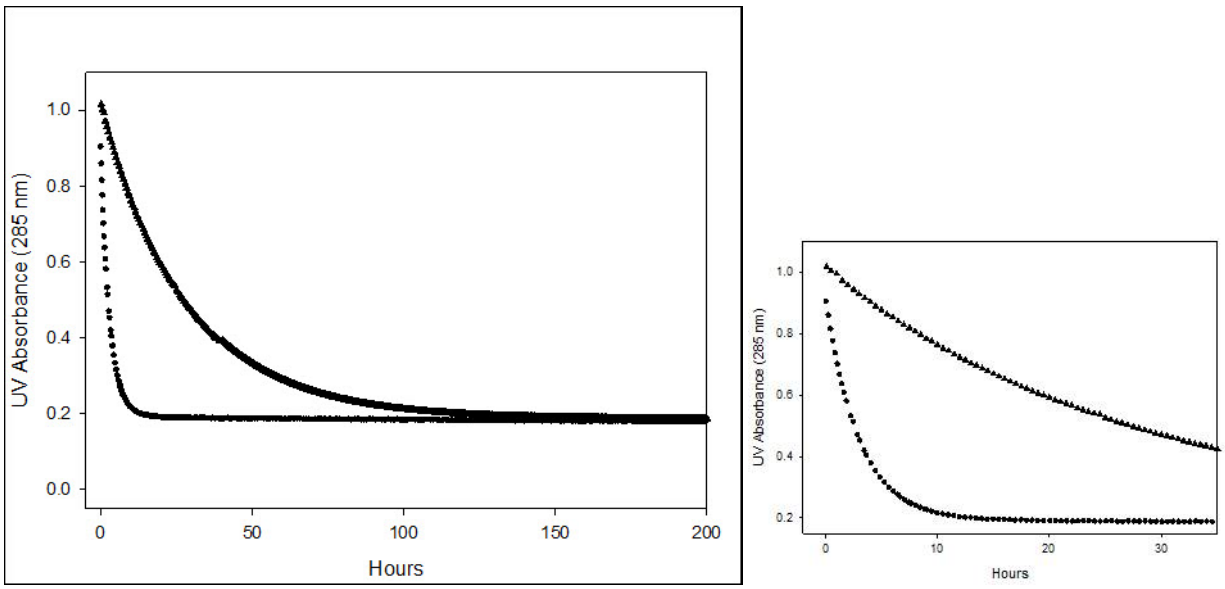

Figure 10. Plot of the total UV absorbance at 285 nm versus time for the reaction of QM with 100 mM Acetate at pH 4 (●) and QM with water without pH adjustment (▲) in 50% (v) aqueous acetonitrile *I* = 0.5 ($NaClO_4$) at 25°C.

The reaction in the presence of acetate buffer does not follow simple first-order kinetics in that the sharp decrease in total absorbance slows down after 5 to 12 hours but the reaction does not reach a stable endpoint. This decrease cannot be accounted for by drift in the UV-Vis instrument reading.

The HPLC chromatograms also show the presence of an apparent adduct peak seen starting almost immediately upon mixing. The adduct peak is formed at the expense of QM and

not BA. After approximately 20 hours, the adduct peak begins to decrease and more BA begins to appear. The adduct peak was assumed to be the acetate adduct of QM because of the increase in the area of the peak at higher concentrations of acetate buffer and higher pH_{app}. The change in the concentration of the acetate adduct displayed in mole fraction, is shown in Figures 6 and 7.

This kinetic behavior of parent and product concentrations can be accounted for by Scheme 5.

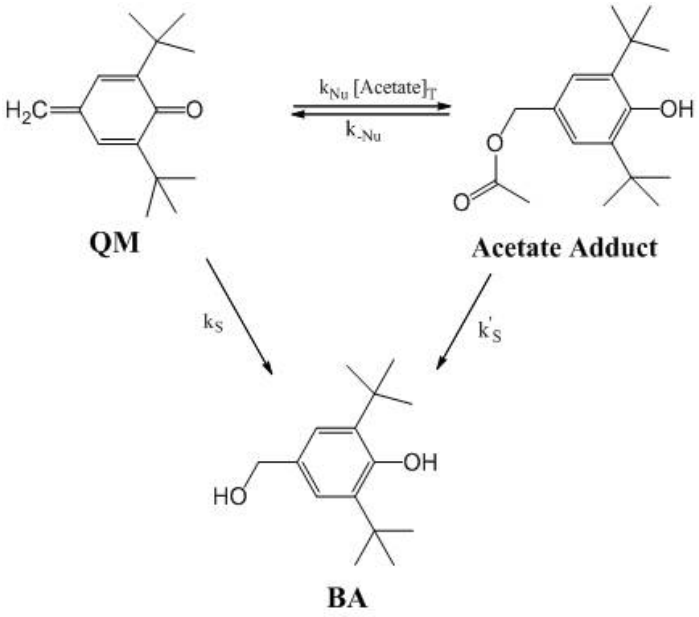

Scheme 5. Proposed formation of the unstable acetate adduct of QM in 50% (v) acetonitrile *I* = 0.5 ($NaClO_4$) and the formation of BA.

The equations for the loss of the QM and the appearance of the acetate adduct based on Scheme 5 can be described by Equations 4-8 [37].

$$QM = \frac{(k_{Nu}[Nu] + k_S - d)QM_0}{b-d} e^{-bt} - \frac{(k_{Nu}[Nu] + k_S - b)QM_0}{b-d} e^{-dt} \qquad \text{(Eq. 4)}$$

$$QMNu = \frac{(k_{Nu}[Nu] + k_S - b)(k_{Nu}[Nu] + k_S - d)QM_0}{k_{-Nu}(b-d)} [e^{-bt} - e^{-dt}] \qquad \text{(Eq. 5)}$$

$$b = (-1/2)\{-(k_{Nu}[Nu] + k_{-Nu} + k_S + k_S') - [(k_{Nu}[Nu] + k_{-Nu} + k_S + k_S')^2 - 4(k_{-Nu}k_S + k_{Nu}[Nu]k_S' + k_S'k_S)]^{1/2}\} \quad \text{(Eq. 6)}$$

$$d = (-1/2)\{-(k_{Nu}[Nu] + k_{-Nu} + k_S + k_S') + [(k_{Nu}[Nu] + k_{-Nu} + k_S + k_S')^2 - 4(k_{-Nu}k_S + k_{Nu}[Nu]k_S' + k_S'k_S)]^{1/2}\} \quad \text{(Eq. 7)}$$

$$b + d = k_{Nu}[Nu] + k_{-Nu} + k_S + k_S' \quad \text{(Eq. 8)}$$

The change in mole fractions of QM and the acetate adduct with time were fit to Equations 9 and 12, respectively. The parameters in Equations 9 and 12 are defined by Equations 10, 11, and 13.

$$y = ae^{-bx} + ce^{-dx} \quad \text{(Eq. 9)}$$

$$a = \frac{(k_{Nu}[Nu] + k_S - d)QM_0}{(b - d)} \quad \text{(Eq. 10)}$$

$$c = \frac{-(k_{Nu}[Nu] + k_S - b)QM_0}{(b - d)} \quad \text{(Eq. 11)}$$

$$y = -z(b - d)[e^{-bx} + e^{-dx}] \quad \text{(Eq. 12)}$$

$$z = \frac{(k_{Nu}[Nu] + k_S - b)(k_{Nu}[Nu] + k_S - d)QM_0}{k_{-Nu}(b - d)} = \frac{-ac(b - d)}{k_{-Nu}QM_0} \quad \text{(Eq. 13)}$$

The UV-Vis data for the initial fast disappearance of QM can be treated as first order. From comparison with the HPLC data, the large change in the total UV absorbance corresponds to the large decrease in the mole fraction of QM. Additionally, QM has a 10-fold larger extinction coefficient than BHT and BA; the same is assumed for the acetate adduct because of its structural similarity to BHT and BA. Thus QM has a dominant contribution to the total UV absorbance at any time point.

The observed first-order rate constants, k_{obs}, were calculated as the slope of the semi-logarithmic plot of the total absorbance versus time. An example of one of these semi-logarithmic plots is shown in the supplemental data. The observed first-order rate constants and the parameters from the non-linear curve fit are shown in Table 6.

Table 6. Table of data fit parameters at various concentrations and pH_{app} values of acetate buffer in 50% (v) aqueous acetonitrile I = 0.5 ($NaClO_4$) for reactions followed by HPLC and UV-Vis at 25°C. Parameters were obtained using Sigma Plot v. 11 software to fit HPLC data in units of mole fraction to Equations 9 and 12. Observed rate constants were calculated from the slope of the semi-logarithmic plot of the loss of UV absorbance at 285 nm versus time.

Acetate		k_{obs}	a	b	c	d	z
0.100 M pH_{app} 3.99	HPLC: QM		0.77 ±0 .04	12.46 ± 1.47	0.23 ± 0.021	0.052 ± 0.0073	
	HPLC: Adduct			11.57 ± 1.55		(3.0 ± 0.1) x 10^{-3}	(7.0 ± 1.0) x 10^{-2}
	UV-Vis	0.32					
0.075 M pH_{app} 3.97	HPLC: QM		0.71 ±0 .04	6.81 ± 0.91	0.29 ± 0.023	0.053 ± 0.0061	
	HPLC: Adduct			6.17 ± 0.97		(3.9 ± 0.2) x 10^{-3}	0.12 ± 0.02
	UV-Vis	0.25					
0.050 M pH_{app} 3.96	HPLC: QM		0.62 ± 0.03	6.52 ± 0.82	0.38 ± 0.021	0.057 ± 0.0041	
	HPLC: Adduct			5.38 ± 0.99		(4.3 ± 0.3) x 10^{-3}	0.13 ± 0.02
	UV-Vis	0.19					
0.100 M pH_{app} 5.02	HPLC: QM		0.90 ±0 .04	16.28 ± 1.80	0.096 ± 0.012	0.010 ± 0.0044	
	HPLC: Adduct			17.66 ± 1.82		(2.2 ± 0.2) x 10^{-3}	0.048 ± 0.005
	UV-Vis	0.42					
0.075 M pH_{app} 5.03	HPLC: QM		0.88 ±0 .04	14.56 ± 1.86	0.12 ± 0.014	0.013 ± 0.0050	
	HPLC: Adduct			16.3 ± 1.67		(2.5 ± 0.2) x 10^{-3}	0.050 ± 0.005
	UV-Vis	0.38					
0.050 M pH_{app} 4.98	HPLC: QM		0.72 ± 0.04	8.61 ± 1.36	0.28 ± 0.031	0.090 ± 0.016	
	HPLC: Adduct			7.44 ± 0.99		(4.3 ± 0.6) x 10^{-3}	0.11 ± 0.01
	UV-Vis	0.26					

The parameters obtained from the non-linear curve fit of the acetate adduct reflect both the loss of QM and the formation and loss of the acetate adduct. From Equation 4, the parameters b and d can be described as the kinetic parameters for the fast and the slow reactions, respectively. There is very good agreement between the value of the parameter b obtained by the non-linear curve fit for the loss of QM and the formation and loss of acetate adduct. However, the values of d obtained the same way differ drastically (Table 6). The b parameter accounts for a large change over a short period of time while the d parameter accounts for a very small change over a much longer period of time. Therefore the fit is always dominated by the value of b. Additionally, any instrument errors or noise would have a larger effect on the smaller reaction parameter, d.

The sum of the non-linear parameters, b + d, is plotted against nucleophile concentration and shown in Figure 11. The dependence is linear as expressed in Equation 8. The slope of this plot is the overall second-order rate constant for the reactions dependent on the nucleophile concentration and the intercept is the overall rate constant for the nucleophile independent reactions.

The parameters from the linear fit (k_{obs}, as determined by the initial UV data) were also plotted versus the nucleophile concentration and shown in Figure 12. The dependence is also linear. The slope of this plot is the observed second-order rate constant for the dependence on nucleophile concentration of the loss of QM.

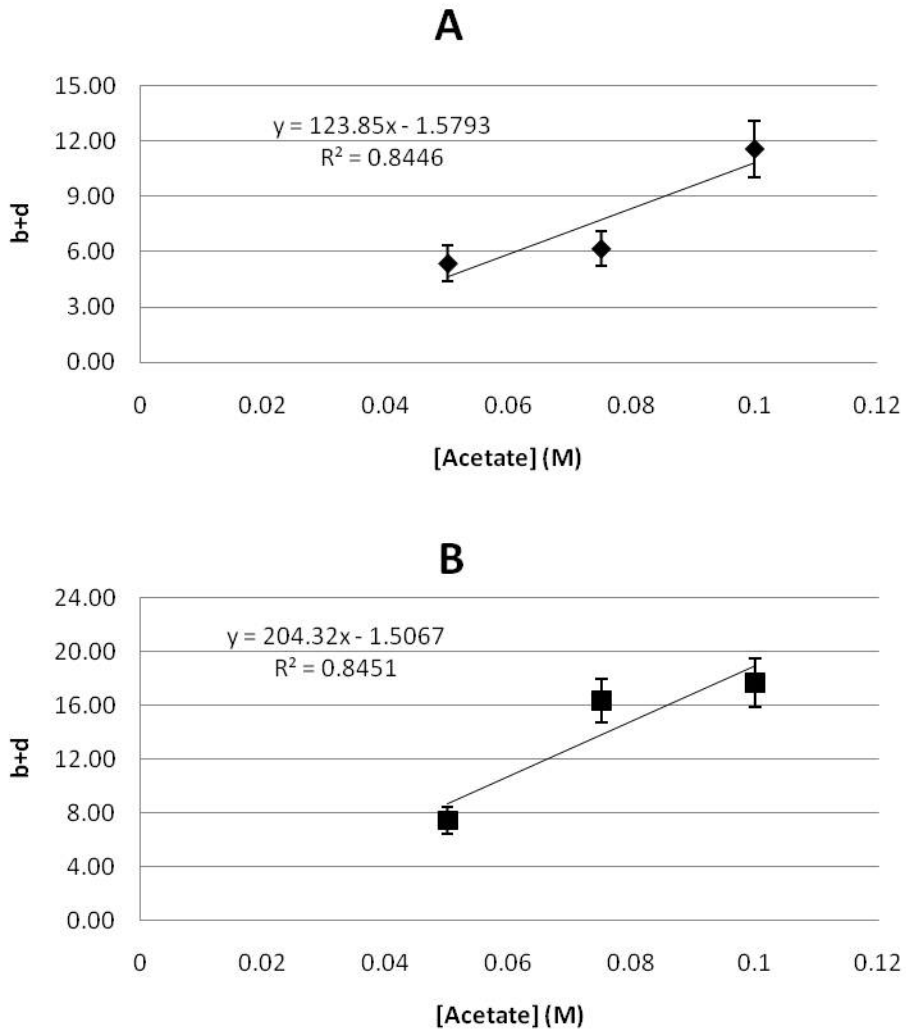

Figure 11. Dependence of observed reaction parameters for the reaction of QM and acetate on concentration of acetate buffer. (A) Data for the sum of b + d obtained as described in text for the reaction pH_{app} 4 (♦). (B) Data for the sum of b + d obtained as described in text for the reaction pH_{app} 5. All reactions run in 50% (v) aqueous acetonitrile *I* = 0.5 ($NaClO_4$) at 25°C.

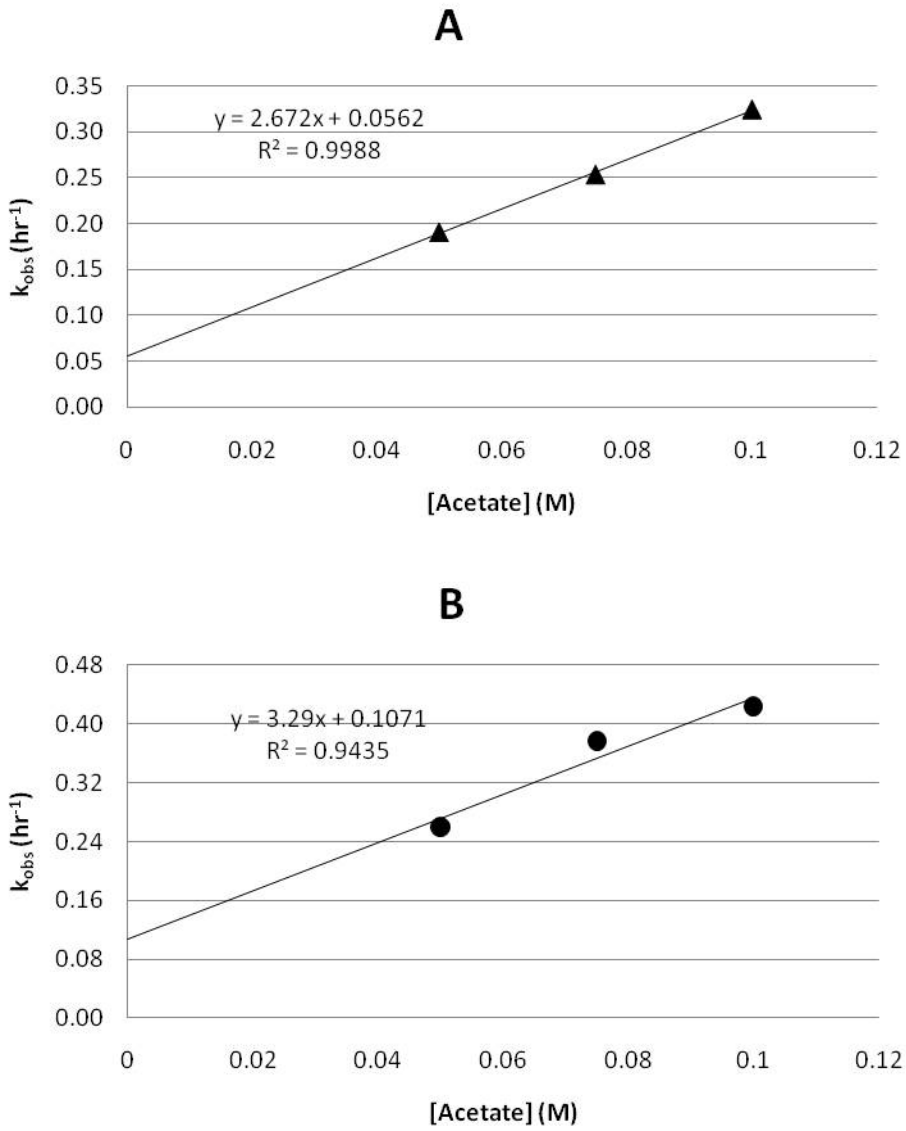

Figure 12. Dependence of observed first-order rate constant for the reaction of QM and acetate on concentration of acetate. (A) Data for the observed first order rate constant, k_{obs}, from the fit of the initial UV-Vis data at pH_{app} 4 (▲). (B) Data for the observed first order rate constant, k_{obs}, from the fit of the initial UV-Vis data at pH_{app} 5 (●). All reactions run in 50% (v) aqueous acetonitrile *I* = 0.5 ($NaClO_4$) at 25°C.

Comparison of the slopes on Figures 11 and 12 show that the dependence of the non-linear curve fit parameters (b + d) on nucleophile concentration is very large compared to the dependence of the observed second-order rate constant for the loss of QM, k_{obs}, at each pH_{app} value. The sum of the non-linear curve fit parameters, (b + d) is 46 and 62 times greater than k_{obs} and pH_{app} 4 and 5, respectively. The additional dependence of (b + d) on the nucleophile concentration indicates the presence of additional kinetic pathways dependent on nucleophile concentration.

The slopes of Figures 11 and 12 are dependent on pH. There is a 65% increase in the slope of the dependence of (b + d) on nucleophile concentration and a 20% increase in the slope of k_{obs} on nucleophile concentration when pH_{app} is increased from 4 to 5.

Both general acid and general base catalysis by acetate buffer on the addition of water to QM can be envisioned (Scheme 6). Additionally both general acid and base catalysis are likely contributors to the breakdown of the acetate adduct, since these mechanisms are common for ester hydrolysis. General base catalysis on the breakdown of the acetate adduct to QM cannot be excluded as well.

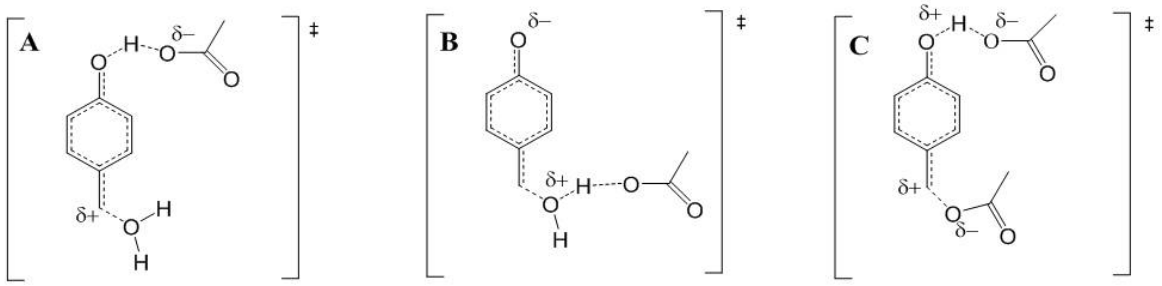

Scheme 6. A) Proposed transition state for general acid catalysis for the addition of water to QM. B) Proposed transition state for general base catalysis for the addition of water to QM. C) Proposed transition state for general base catalysis on the breakdown of the acetate adduct to QM.

In order to reflect the large dependence of the reaction on acetate and to include terms for the general acid and base catalysis of the reaction by acetate Scheme 5 was amended to Scheme 7.

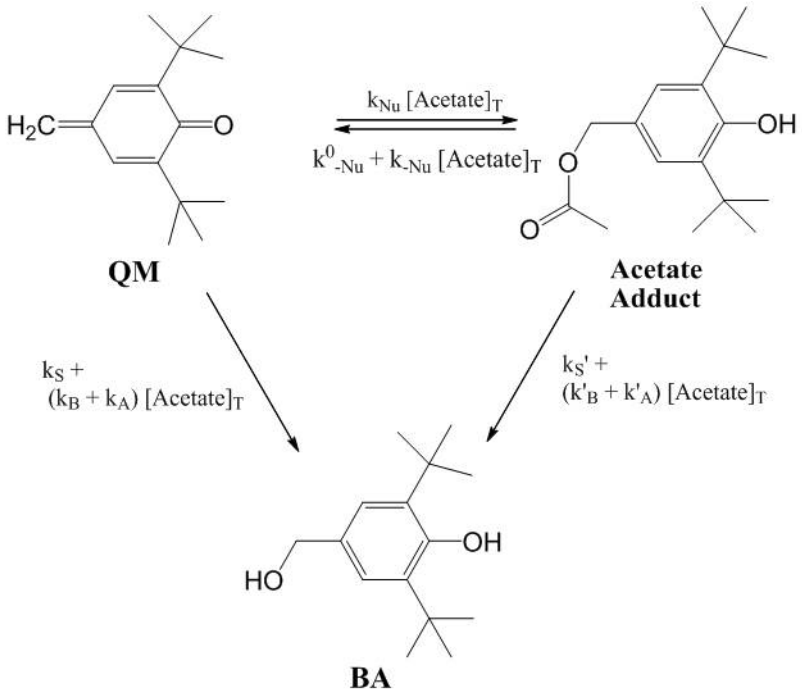

Scheme 7. Proposed scheme for the formation of the unstable acetate adduct of QM in 50% (v) acetonitrile *I* = 0.5 ($NaClO_4$) and the formation of BA.

For Scheme 7, b + d is given by Equation 14.

$$b + d = (k_{Nu} + k_{-Nu} + k_A + k_B + k'_A + k'_B)[Nu] + k_S + k'_S + k^0_{-Nu} \qquad \text{(Eq. 14)}$$

Where k_A, k_B, k'_A, and k'_B are the second-order rate constants for general acid and base catalysis of QM and the acetate adduct, respectively and k^0_{-Nu} is the first-order rate constant for the uncatalyzed breakdown of the acetate adduct to QM.

Reaction of QM in the Presence of TAPS Buffers

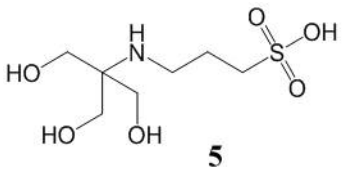

5

TAPS, **5**, is a common laboratory buffer with three possible nucleophilic groups. The reaction of QM in the presence of TAPS buffer shows an initial decrease in total absorbance that is very rapid compared to the reaction with water and similar to that seen with the acetate data. The initial decrease in total absorbance for the reaction in the presence of TAPS buffer is approximately 12 to 36 times faster than the reaction with water.

Like for acetate, the reaction in the presence of TAPS buffer is also not simple first-order kinetics in that the sharp decrease in total absorbance slows down after approximately 2 to 8 hours, depending on pH_{app} and TAPS buffer concentration, but the reaction does not reach a stable endpoint. This decrease cannot be accounted for by drift in the instrument reading.

Surprisingly, no additional product peaks could be detected in the method used besides that water addition product, BA. Careful examination of the solvent front peak did not show any obvious additional peaks. However, mass balance cannot be satisfied by the concentration of QM and BA, that is, a significant portion of the mass is missing. The HPLC data displayed in mole fractions is shown in Figures 8 and 9 in the results section, the fraction of missing mass is also included.

TAPS contains three nucleophilic groups that could possibly form adducts with QM; a secondary amine, sulfonic acid, and three primary alcohols. Adduct formation with the secondary amine is most likely, however, addition of sulfonate to a quinone methide (quinone methide **4**) has been reported [38]. Adduct formation with the primary alcohols is possible but

would most likely have to compete with the addition of water. The extinction coefficients of all the possible adduct structures would be assumed to be approximately 10 fold smaller than that of QM and similar to those of other substituted phenols including BHT itself and BA. Additionally, all the possible adduct structures would be quite polar and would most likely elute with the solvent front. Considering these factors combined with the unknown stability of the three possible adducts, it is not surprising that no adducts could be detected by this HPLC analysis during the course of the experiment. Changes to the chromatographic conditions could make possible the detection and quantitation of the small polar adducts. Scheme 8 was proposed.

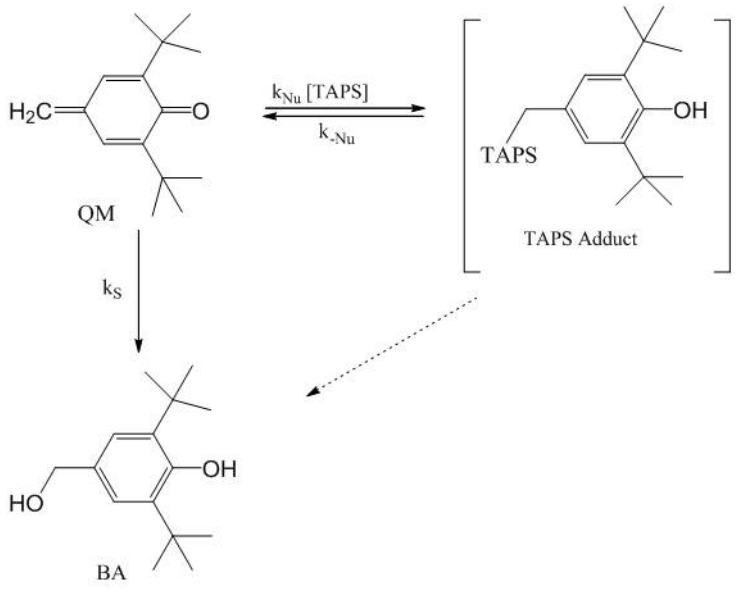

Scheme 8. Proposed formation of an unstable TAPS adduct of QM in 50% (v) acetonitrile *I* = 0.5 ($NaClO_4$) and the formation of BA.

For Scheme 8, the exact equations for the loss of the QM can be described by Equations 4, and 6-8 where the k_s' could be equal to zero [37]. The change in mole fractions of QM with time was fit to Equation 9. The parameters in Equation 9 are defined by Equations 10 and 11.

The UV-Vis data for the initial fast disappearance of QM can be treated as approximately first order. From comparison with the HPLC data, the large change in the total UV absorbance corresponds to the large decrease in the mole fraction of QM. Additionally, QM has a 10-fold larger extinction coefficient than BHT and BA; the same is assumed for any TAPS adducts. Thus QM has a dominant contribution to the total UV absorbance at any time point.

The observed first-order rate constants, k_{obs}, were calculated as the slope of the semi-logarithmic plot of the total absorbance versus time. An example of one of these semi-logarithmic plots is shown in the supplemental data. The observed first-order rate constants and the parameters from the non-linear curve fit are shown in Table 7.

Table 7. Table of data fit parameters at various concentrations and pH_{app} values of TAPS buffer in 50% (v) aqueous acetonitrile I = 0.5 ($NaClO_4$) for reactions followed by HPLC and UV-Vis at 25°C. Parameters were obtained using Sigma Plot v. 11 software to fit HPLC data in units of mole fraction to Equation 9. Observed rate constants were calculated from the slope of the semi-logarithmic plot of the loss of UV absorbance at 285 nm versus time.

TAPS		k_{obs}	a	b	c	d
0.100 M pH_{app} 8.05	HPLC: QM		0.94 ± 0 .006	19.01 ± 0.36	0.058 ± 0.002	0.0081 ± 0.001
	UV-Vis	0.97				
0.075 M pH_{app} 8.03	HPLC: QM		0.93 ± 0.008	18.6 ± 0.46	0.072 ± 0.003	0.0091 ± 0.001
	UV-Vis	0.86				
0.050 M pH_{app} 8.02	HPLC: QM		0.90 ± 0 .01	14.94 ± 0.55	0.10 ± 0.005	0.014 ± 0.002
	UV-Vis	0.65				
0.100 M pH_{app} 8.98	HPLC: QM		0.91 ± 0 .002	10.2 ± 0.063	(9.0 ± 0.8) x 10^{-3}	(2.0 ± 0.4) x 10^{-3}
	UV-Vis	1.90				
0.075 M pH_{app} 8.97	HPLC: QM		0.89 ± 0 .005	7.41 ± 0.12	0.11 ± 0.002	0.023 ± 0.001
	UV-Vis	1.55				
0.050 M pH_{app} 8.96	HPLC: QM		0.86 ± 0 .005	7.64 ± 0.13	0.14 ± 0.002	(2.3 ± 0.8) x 10^{-3}
	UV-Vis	1.23				

Since no adduct peaks were detected it is not possible to compare the UV and HPLC mole fraction data directly. The observed first-order rate constants, as determined by the initial UV data, were also plotted versus the concentration of nucleophile in Figure 13. The slope of this plot is the observed second-order rate constant for the loss of QM in the presence of TAPS.

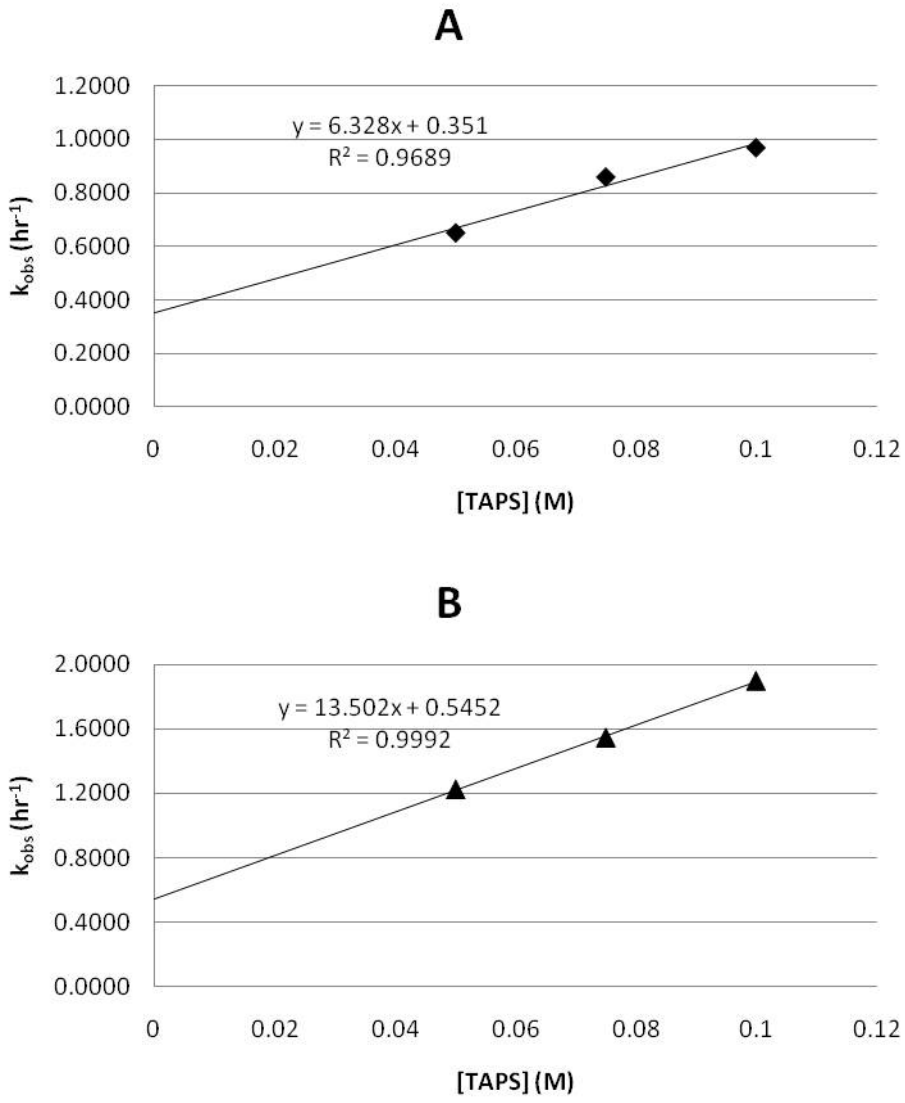

Figure 13. Dependence of observed first order rate constant, k_{obs}, from the fit of the initial UV-Vis data for the reaction of QM in the presences of TAPS on the concentration of TAPS buffer. (A) Data for the reaction at pH_{app} 8 (♦). (B) Data for the reaction at pH_{app} 9 (▲). All reactions run in 50% (v) aqueous acetonitrile *I* = 0.5 ($NaClO_4$) at 25°C.

Comparing the rate constants from A and B in figure 13 shows a effect of pH on the dependence of the observed first-order rate constants on TAPS buffer concentration. The apparent second-order rate constant for the loss of QM as measured by the initial UV data is 2 fold larger at pH_{app} 9 than at pH_{app} 8.

TAPS contains two ionizable groups; a secondary amine and sulfonic acid and has an aqueous pKa of 8.4 [39]. At pH_{app} 8, the zwitterion species is dominant, at pH_{app} 9, the negative sulfonate ions are the dominant ionized species. Due to the large pH effect, it is possible to reasonably conclude that QM reacts more rapidly in the presence of the negatively charged TAPS ion than in the presence of the neutral zwitterion.

Comparison of QM reactivity to other Quinone Methides

There is a large amount of data published on the reactivity of structurally similar quinone methides with nucleophiles.

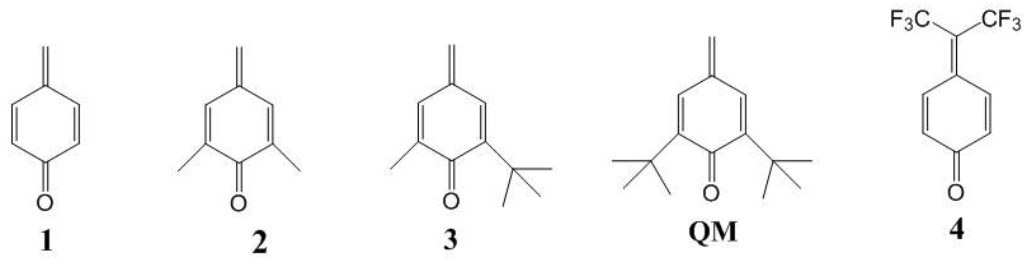

Some relevant rate constants for these quinone methides are shown in Table 8.

Table 8. First and second-order rate constants for the reactions of various quinone methides with nucleophiles. Observed first-order constants reported in hr^{-1}, observed second-order rate constants reported as $hr^{-1}M^{-1}$.

	Solvent	**1**	**2**	**3**	**QM**	**4**	Reference
k_s hr^{-1}	ACN/H_2O 20/80 pH = 7.4 (Phos)		96	53	0.18		[29]
	ACN/H_2O 50/50 *I* = 0.5 ($NaClO_4$)				0.053		
	H_2O *I* = 0.1 ($NaClO_4$)	1.2×10^4					[40]
	H_2O *I* = 1 ($NaClO_4$)					2.3	[38]
	TFE/H_2O 50/50 *I* = 0.5 ($NaClO_4$)					0.061	[41]
k_H $hr^{-1}M^{-1}$	ACN/H_2O 50/50 *I* = 0.5 ($NaClO_4$)				2.87×10^3		
	H_2O *I* = 0.1 ($NaClO_4$)	1.9×10^8					[40]
	H_2O *I* = 1 ($NaClO_4$)					75.6	[38]
	TFE/H_2O 50/50 *I* = 0.5 ($NaClO_4$)					12	[41]
k_{Cl} $hr^{-1}M^{-1}$	ACN/H_2O 50/50 *I* = 0.5 ($NaClO_4$)				NR		
	H_2O *I* = 0.1 ($NaClO_4$)	4.0×10^6					[40]
	H_2O *I* = 1 ($NaClO_4$)					576	[38]
$k_{AcetApp}$ = (k_{Acet} + k_B) $hr^{-1}M^{-1}$	ACN/H_2O 50/50 *I* = 0.5 ($NaClO_4$) pH 4				2.6		
	H_2O *I* = 1 ($NaClO_4$)					176.4	[38]

NR: no adduct was observed

The simplest *p*-quinone methide, **1**, was recently generated by flash photolysis [40] and found to be highly reactive with a half-life of 0.2 seconds in aqueous solvents. Adding substituents at the 2 and 6 positions greatly enhance the stability of the quinone methide as can be seen in the significantly reduced rate constant for the addition of water for **1** and **2** respectively. The dimethyl (**2**), methyl, *t*-butyl (**3**), and di-*t*-butyl (QM) 2, 6-substituted quinone methides have a trend of decreasing reactivity with increased size of aliphatic substituents. The addition of a single *t*-butyl group almost doubles the half-life from 26 to 48 seconds; however,

replacing the methyl group of **3** with an additional *t*-butyl substituent increases the half-life 65-fold to 3060 seconds.

The greater enhancement in stability of QM versus quinone methides **2** and **3** has been attributed to steric hindrance [29]. The large *t*-butyl groups at the 2 and 6 positions effectively block solvent interactions and therefore, the stabilization of the partially negative charge on the phenoxyl oxygen. This increases the delocalization of the charge into the quinone methide structure leading to greater stability.

Another possible contribution to the stabilization of QM can come from the distortion of the geometry or planarity of the quinone methide structure by the bulky *t*-butyl groups. This distorted geometry would create a greater barrier to the delocalization of the electrons in the aromatic product of nucleophilic addition.

In 50% (v) aqueous solvent systems QM has similar reactivity to quinone methide **4**. The unsubstituted ring structure of **4** would lead to the assumption that it would be highly reactive but that is not the case. Researchers concluded that the trifluoro-methyl substituents on the methylene carbon decreased the bipolar nature of the molecule by increasing delocalization of the charge into the quinone methide structure and therefore increasing the intrinsic kinetic barrier for its reaction [38]. This is essentially the same argument made for the greater stability of QM.

The reactivity of **4** is 35-40 fold higher in a fully aqueous environment with higher ionic strength. This same effect is seen in the two reported values for the observed first-order rate constant of QM for the addition of water. The previously published value is three fold larger and was obtained in a more aqueous solvent system than the value obtained in these experiment.

Chloride adducts to **1** and **4** have been observed and the kinetic and thermodynamic parameters of the reactions have been reported [38, 40]. Both of the above reactions were carried out in the presence of acid which stabilizes the chloride adduct of the quinone methide. In the work reported here, a chloride adduct was not observed at neutral pH_{app} values and it is possible that a chloride adduct between QM could be observed at lower pH values but that was not likely since no differences were seen for the reactivity of QM in perchloric acid versus hydrochloric acid in our studies. At concentrations of 0.005 to 0.010 M acid, the rate constant for the addition of water did not depend on the counter ion of the acid. This data leads to the conclusion that in this concentration range of chloride and acid, a chloride adduct was not formed to any significant extent.

The effect of alkyl phosphates and inorganic phosphate on the rate of disappearance of the quinone methide **2** have been reported in the literature [42]. A stable adduct was observed between **2** and diethyl phosphate in the presence of acid but it was not specified if an adduct to inorganic phosphate was observed. Based on comparison of the reported rate constants for the addition of water and the observed rate constant in the presence of inorganic phosphate, we conclude that a phosphate adduct was not formed to any significant extent. At pH_{app} 7 the observed first-order rate constant from the reaction of **2** in the presence of inorganic phosphate increased 50%. However, no further experiments were done to determine if the difference in rate constant at the two pH_{app} values was due to the change in pH or the effect of phosphate.

A stable acetate adduct to **4** has been reported [38]. The acetate adduct was stable when formed in dilute solutions of **4** (1×10^{-5} M), but at higher concentrations it reacted with a second molecule of **4** to give a dimeric product. An observed second-order rate constant, ($k_{Acet} + k_B$) = 176.4 hr^{-1} M^{-1}, for the reaction of dilute solutions of **4** in the presence of acetate was reported,

where k_{Acet} = 172.8 is the contribution of the nucleophilic addition of acetate and k_B = 3.6 is the contribution of general base catalysis. The second-order rate constant k_{Acet} for **4** is much larger than the observed second-order rate constant for the QM ($k_{Acet} + k_B$) = 2.6 although the reactivity of both quinone methides towards addition of solvent is similar (Table 8). This results in significantly higher selectivity (k_{Acet}/k_s) for **4** compared to QM, and indicates that **4** is the more stable electrophile.

At physiological conditions, the observed rate-constants of QM with nucleophiles is expected to be greater, since a 35-40 fold increase in rate constant was seen for the addition of water to **4** when the reaction was examined in a fully aqueous environment versus 50% (v) aqueous environment (Table 8). Similar effect of solvent on k_s for reaction of QM was also observed (Table 8).

Conclusions

BHT is widely used as an antioxidant in many industries and is present at low levels in several marketed pharmaceutical formulations and some foods. Published data shows when BHT is oxidized to QM, which can form adducts with DNA *in vitro*, however, there is no literature on the reactivity of QM with common nucleophiles present in excipients, API molecules, buffers, and biological molecules present at the site of QM formation through biotransformation.

The reactivity of QM was examined with water in the presence of acid, base, chloride, phosphate, acetate, and TAPS. The reaction with water resulted in a single product, BA. BA is formed through the addition of water to the highly electrophilic methylene carbon of the quinone methide. This reaction was catalyzed by the presence of both added acid and base (hydroxide ions). However, the presence of added chloride and phosphate had little effect on the reaction.

QM reacted very quickly with acetate to form an apparent acetate adduct that was unstable and subsequently hydrolyzed to form BA. The kinetics of the reaction were complicated and non-linear curve fits were used to analyze the data. The reaction of QM in the presence of TAPS also resulted in complicated kinetics. The loss of QM was similar to that seen in the reaction with acetate however a TAPS adduct was not detected.

Additional studies could be undertaken to fully understand the reactivity of QM with a variety of additional nucleophiles and extend the work reported here. The study of reactions with chloride and phosphate could be extended to acidic conditions to see if the presence of acid catalyzes and stabilizes adduct formation and detection. However, this would be technically challenging due to the reactivity of QM with whatever component is used to control the pH.

The reaction with acetate could be studied at additional pH values to better understand the affects of general acid and base catalysis. In addition, the reaction with TAPS could be studied at additional pH values using an HPLC method more likely to detect the possible adducts, which could not be detected by the present HPLC method. Finally, the kinetics of reactions of QM with excipients and API molecules containing nucleophilic groups could be explored and the products identified. This work could be done in solution and the most reactive cases could also be investigated in the solid state.

Understanding the reactivity of QM with these nucleophiles has consequences for the use of BHT in pharmaceutical formulations. This work has shown that QM reacts readily with water and a pharmaceutically relevant buffer. The formation of an apparent acetate adduct occurred very rapidly, however, due to the instability of the adduct and the equilibria of the system, small amounts of QM where still in solution for a much longer time period than would be expected for the addition of water to QM.

The prolonged levels of QM present in a drug product would risk additional reactivity with other nucleophilic groups. QM adducts formed through interaction between QM and nucleophiles in the drug product would be considered degradants and would need to be reported and identified depending on the amount generated, requiring additional regulatory submissions and the development of new analytical methods. Additionally, very small amounts of these possible degradants could change the color or odor of the drug product leading to a shorter shelf-life.

In addition to QM reacting with nucleophiles in the drug product it has also been shown to react with nucleophilic groups found in the body [29, 31-33]. No safe level of exposure to QM has been established for humans. The introduction of QM into the body as an oxidation product in the drug product or through the biotransformation of BHT to QM *in vivo* could lead to adduct formation with biological molecules including DNA. The consequences of repeated exposure are unknown but could include cellular toxicity that could lead to the development of tumors.

The reactivity of QM at physiological conditions or fully aqueous environment would be expected to be greater than the reactivity shown in this work in 50% (v) aqueous solutions. The effect of competition from additional nucleophilic groups present *in vivo* could also greatly impact these reactions. Due to all of these factors and unknowns, BHT should be used with caution as a pharmaceutical antioxidant.

References

1. Babich, H., *Butylated hydroxytoluene (BHT): a review.* Environ. Res., 1982. **29**(1): p. 1-29.
2. Stebbins, R. and F. Sicilio, *Kinetics of disproportionation of the 2,6-di-tert-butyl-4-methyl phenoxy radical.* Tetrahedron, 1970. **26**(1): p. 291-7.
3. Zhang, F. and M. Nunes, *Structure and generation mechanism of a novel degradation product formed by oxidatively induced coupling of miconazole nitrate with butylated hydroxytoluene in a topical ointment studied by HPLC-ESI-MS and organic synthesis.* J. Pharm. Sci. FIELD Full Journal Title:Journal of Pharmaceutical Sciences, 2004. **93**(2): p. 300-309.
4. Toteva, M.M., et al., *Substituent Effects on Carbocation Stability: The pKR for p-Quinone Methide.* J. Am. Chem. Soc., 2003. **125**(29): p. 8814-8819.
5. Wagner, H.-U.a.G., R., *Quinone methides*, in *The Chemistry of Quinoid Compounds*, S. Patai, Editor. 1974, Wiley & Sons: New York. p. 1145-1178.
6. Fan, P.W. and J.L. Bolton, *Bioactivation of tamoxifen to metabolite E quinone methide: reaction with glutathione and DNA.* Drug Metab. Dispos., 2001. **29**(6): p. 891-896.
7. Liu, J., et al., *Bioactivation of the Selective Estrogen Receptor Modulator Acolbifene to Quinone Methides.* Chem. Res. Toxicol., 2005. **18**(2): p. 174-182.
8. Wang, P., et al., *Quinone methide derivatives: Important intermediates to DNA alkylating and DNA cross-linking actions.* Curr. Med. Chem., 2005. **12**(24): p. 2893-2913.
9. Leary, G.J., *Quinone methides and the structure of lignin.* Wood Sci. Technol., 1980. **14**(1): p. 21-34.

10. Shevchenko, S.M. and A.G. Apushkinskii, *Quinonemethides in wood chemistry.* Usp. Khim., 1992. **61**(1): p. 195-245.

11. Wan, P., et al., *1995 Merck Frosst Award Lecture. Quinone methides: relevant intermediates in organic chemistry.* Can. J. Chem., 1996. **74**(4): p. 465-475.

12. Kehrer, J.P. and H. Witschi, *The effect of indomethacin, prednisolone and cis-4-hydroxyproline on pulmonary fibrosis produced by butylated hydroxytoluene and oxygen.* Toxicology, 1981. **20**(4): p. 281-8.

13. Chapman, O.L., et al., *Total synthesis of carpanone.* J. Amer. Chem. Soc., 1971. **93**(24): p. 6696-8.

14. Marino, J.P. and S.L. Dax, *An efficient desilylation method for the generation of o-quinone methides: application to the synthesis of (+)- and (-)-hexahydrocannabinol.* J. Org. Chem., 1984. **49**(19): p. 3671-2.

15. Genisson, Y. and R.N. Young, *Practical total synthesis of a naturally occurring thielocin via the regioselective arylation of a cyclic boronate.* Tetrahedron Lett., 1994. **35**(42): p. 7747-50.

16. Genisson, Y., P.C. Tyler, and R.N. Young, *Total synthesis of (+-)-thielocin A1beta : a novel inhibitor of phospholipase A2.* J. Am. Chem. Soc., 1994. **116**(2): p. 759-60.

17. Filar, L.J. and S. Winstein, *Preparation and behavior of simple quinone methides.* Tetrahedron Lett., 1960(No. 25): p. 9-16.

18. Bennett, J.E., *Study by electron spin resonance of the oxidation of hindered phenols.* Nature (London, U. K.), 1960. **186**: p. 385-6.

19. Bauer, R.H. and G.M. Coppinger, *Chemistry of hindered phenols. Reactivity of 2,6-di-tert-butyl-4-methylphenoxyl.* Tetrahedron, 1963. **19**(8): p. 1201-6.

20. Witschi, H., D. Williamson, and S. Lock, *Enhancement of urethan tumorigenesis in mouse lung by butylated hydroxytoluene.* J. Natl. Cancer Inst., 1977. **58**(2): p. 301-5.

21. Takahashi, O. and K. Hiraga, *Dose-response study of hemorrhagic death by dietary butylated hydroxytoluene (BHT) in male rats.* Toxicol. Appl. Pharmacol., 1978. **43**(2): p. 399-406.

22. Takahashi, O., et al., *Short-term toxicity of butylated hydroxytoluene in mice.* Tokyo-toritsu Eisei Kenkyusho Kenkyu Nempo, 1979(30-2): p. 1-4.

23. Takahashi, O., T. Nakao, and K. Hiraga, *Hemorrhages in aged rats caused by dietary butylated hydroxytoluene (BHT).* Tokyo-toritsu Eisei Kenkyusho Kenkyu Nempo, 1979(30-2): p. 22-4.

24. Takahashi, O. and K. Hiraga, *2,6-Di-tert-butyl-4-methylene-2,5-cyclohexadienone: a hepatic metabolite of butylated hydroxytoluene in rats.* Food Cosmet. Toxicol., 1979. **17**(5): p. 451-4.

25. Witschi, H.P., *Enhanced tumor development by butylated hydroxytoluene (BHT) in the liver, lung and gastro-intestinal tract.* Food Chem. Toxicol., 1986. **24**(10-11): p. 1127-30.

26. Witschi, H., A.M. Malkinson, and J.A. Thompson, *Metabolism and pulmonary toxicity of butylated hydroxytoluene (BHT).* Pharmacol. Ther., 1989. **42**(1): p. 89-113.

27. Marino, A.A. and J.T. Mitchell, *Lung damage in mice following intraperitoneal injection of butylated hydroxytoluene.* Proc. Soc. Exp. Biol. Med., 1972. **140**(1): p. 122-5.

28. Mizutani, T., et al., *Pulmonary toxicity of butylated hydroxytoluene and related alkylphenols: structural requirements for toxic potency in mice.* Toxicol. Appl. Pharmacol., 1982. **62**(2): p. 273-81.

29. Bolton, J.L., L.G. Valerio, Jr., and J.A. Thompson, *The enzymic formation and chemical reactivity of quinone methides correlate with alkylphenol-induced toxicity in rat hepatocytes.* Chem. Res. Toxicol. FIELD Full Journal Title:Chemical Research in Toxicology, 1992. **5**(6): p. 816-22.

30. Wang, H. and S.E. Rokita, *Dynamic Cross-Linking Is Retained in Duplex DNA after Multiple Exchange of Strands.* Angew. Chem., Int. Ed., 2010. **49**(34): p. 5957-5960, S5957/1-S5957/3.

31. Bolton, J.L. and L. Shen, *p-Quinone methides are the major decomposition products of catechol estrogen o-quinones.* Carcinogenesis, 1996. **17**(5): p. 925-929.

32. Nakagawa, Y., K. Hiraga, and T. Suga, *Biological fate of butylated hydroxytoluene (BHT). Binding of BHT to nucleic acid in vivo.* Biochem. Pharmacol., 1980. **29**(9): p. 1304-6.

33. Sato, H., et al., *Initiating potential of 2-(2-furyl)-3-(5-nitro-2-furyl)acrylamide (AF-2), butylated hydroxyanisole (BHA), butylated hydroxytoluene (BHT) and 3,3',4',5,7-pentahydroxyflavone (quercetin) in two-stage mouse skin carcinogenesis.* Cancer Lett. (Shannon, Irel.), 1987. **38**(1-2): p. 49-56.

34. Bolton, J.L., S.B. Turnipseed, and J.A. Thompson, *Influence of quinone methide reactivity on the alkylation of thiol and amino groups in proteins: studies utilizing amino acid and peptide models.* Chem.-Biol. Interact. FIELD Full Journal Title:Chemico-Biological Interactions, 1997. **107**(3): p. 185-200.

35. Bolton, J.L., et al., *Formation and reactivity of alternative quinone methides from butylated hydroxytoluene: possible explanation for species-specific pneumotoxicity.*

Chem. Res. Toxicol. FIELD Full Journal Title:Chemical Research in Toxicology, 1990. **3**(1): p. 65-70.

36. Sedlacek, B., *Ultraviolet spectra of antioxidants. I. The influence of solvents and fat rancidity on the spectra.* Fette, Seifen, Anstrichm., 1962. **64**: p. 683-7.

37. Alberty, R.A. and W.G. Miller, *Integrated rate equations for isotopic exchange in simple reversible reactions.* J. Chem. Phys., 1957. **26**: p. 1231-7.

38. Richard, J.P., M.M. Toteva, and J. Crugeiras, *Structure-Reactivity Relationships and Intrinsic Reaction Barriers for Nucleophile Additions to a Quinone Methide: A Strongly Resonance-Stabilized Carbocation.* J. Am. Chem. Soc., 2000. **122**(8): p. 1664-1674.

39. Goldberg, R.N., N. Kishore, and R.M. Lennen, *Thermodynamic quantities for the ionization reactions of buffers.* J. Phys. Chem. Ref. Data, 2002. **31**(2): p. 231-370.

40. Chiang, Y., A.J. Kresge, and Y. Zhu, *Flash Photolytic Generation and Study of p-Quinone Methide in Aqueous Solution. An Estimate of Rate and Equilibrium Constants for Heterolysis of the Carbon-Bromine Bond in p-Hydroxybenzyl Bromide.* J. Am. Chem. Soc., 2002. **124**(22): p. 6349-6356.

41. Richard, J.P., *Mechanisms for the uncatalyzed and hydrogen ion catalyzed reactions of a simple quinone methide with solvent and halide ions.* J. Am. Chem. Soc., 1991. **113**(12): p. 4588-95.

42. Zhou, Q. and K.D. Turnbull, *Quinone Methide Phosphodiester Alkylations under Aqueous Conditions.* J. Org. Chem., 2001. **66**(21): p. 7072-7077.

Appendix: Supplemental Data

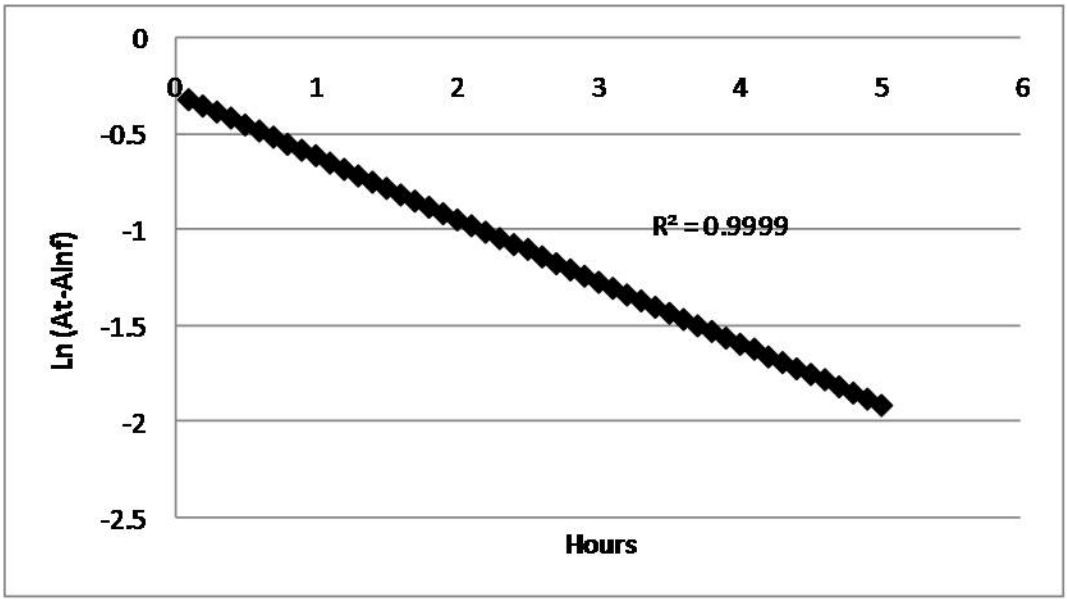

Supplemental Data Figure 2. A semi logarithmic plot of the loss of total absorbance versus time over two and a half half-lives. Data for reaction of QM in 0.100 M Acetate pH_{app} 4 (♦) 50% (v) aqueous acetonitrile *I* = 0.5 ($NaClO_4$) at 25°C.

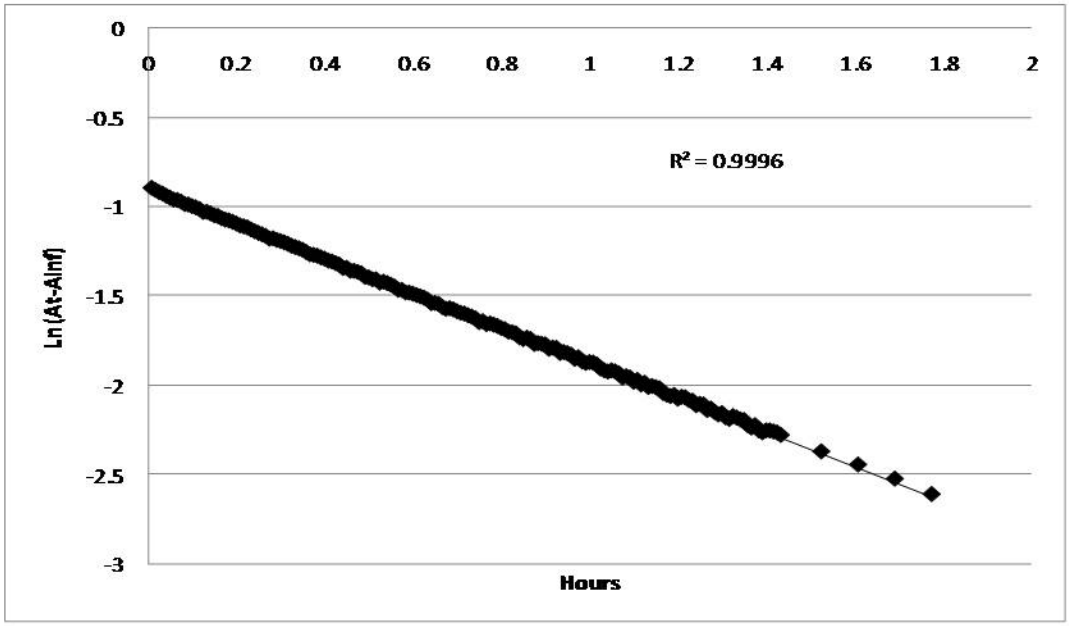

Supplemental Data Figure 3. A semi logarithmic plot of the loss of total absorbance versus time over two and a half half-lives. Data for reaction of QM in 0.100 M TAPS pH_{app} 8 (♦) 50% (v) aqueous acetonitrile *I* = 0.5 ($NaClO_4$) at 25 °C.